Simulation of the tropospheric sulfur cycle in a global model with a physically based cloud scheme

Leon D. Rotstayn

Division of Atmospheric Research, CSIRO, Aspendale, Victoria, Australia

Ulrike Lohmann

Department of Physics and Atmospheric Science, Dalhousie University, Halifax, Nova Scotia, Canada

[1]   The treatment of the sulfur cycle in the CSIRO global climate model (GCM) is described. It is substantially based on the scheme developed previously for the European Center/Hamburg (ECHAM) model, but the treatment of wet scavenging has been completely rewritten to better reflect the different properties of liquid and frozen precipitation, and the treatment of these in the model's cloud microphysical scheme. The model is able to reproduce the observed finding that wet deposition of sulfur over Europe and North America is larger in summer than in winter, but the seasonal cycle of sulfate over Europe is not well simulated. The latter is improved when the amplitude of the seasonal cycle of European emissions is increased. Below-cloud scavenging makes an important contribution in our scheme: On omitting it, the global sulfate burden increases from 0.67 to 0.93 Tg S. On reverting to the less efficient scavenging treatment used in ECHAM, the global sulfate burden again increases from 0.67 to 0.93 Tg S, and excessive sulfate concentrations are obtained in Europe and North America. Some deficiencies in the simulation are investigated via further sensitivity tests. In particular, during the Arctic winter, the modeled sulfur dioxide (SO_2) concentrations are too large, and the modeled sulfate concentrations are too small (as in most global sulfur-cycle models). Recent laboratory experiments suggest that SO_2 oxidation in ice clouds is nonnegligible. We obtain a much improved Arctic simulation when a simple treatment of SO_2 oxidation in ice clouds is included.   *INDEX TERMS:* 0305 Atmospheric Composition and Structure: Aerosols and particles (0345, 4801); 0320 Atmospheric Composition and Structure: Cloud physics and chemistry; 3337 Meteorology and Atmospheric Dynamics: Numerical modeling and data assimilation; *KEYWORDS:* sulfur cycle, global climate model, sulfate aerosol, scavenging, cloud, precipitation

1. Introduction

[2] The direct and indirect radiative effects of sulfate aerosol are now recognized as important factors driving global climate change [e.g., *Haywood and Boucher*, 2000]. Partly for this reason, a range of global models have been used to study the tropospheric sulfur cycle during the last decade or so [*Langner and Rodhe*, 1991; *Penner et al.*, 1994; *Pham et al.*, 1995; *Feichter et al.*, 1996; *Chin et al.*, 1996, 2000a, 2000b; *Kasibhatla et al.*, 1997; *Lelieveld et al.*, 1997; *Roelofs et al.*, 1998; *Adams et al.*, 1999; *Koch et al.*, 1999; *Lohmann et al.*, 1999b; *Barth et al.*, 2000; *Rasch et al.*, 2000a]. Some of these models have been driven by offline winds derived from a global climate model (GCM) or analyzed meteorology, and others have been incorporated directly into GCMs. Modeling of the sulfur cycle is still considered very uncertain in many respects, as is empha-sized by the results of a recent intercomparison of 11 sulfur-cycle models [*Barrie et al.*, 2001; *Lohmann et al.*, 2001; *Roelofs et al.*, 2001]. A measure of the uncertainty is that the sulfate burdens simulated by these models differ by a factor of more than two [*Roelofs et al.*, 2001]. One specific factor that has been identified as contributing to this uncertainty is the treatment of wet scavenging processes [e.g., *Rasch et al.*, 2000b].

[3] Even more uncertain are the indirect effects of sulfate (and other) aerosols, whereby cloud properties are modified by anthropogenic aerosols. The "first indirect effect" refers to the radiative impact of a decrease in droplet effective radius that results from increases in aerosols [*Twomey*, 1977]. The "second indirect effect" refers to the radiative impact of a decrease in precipitation efficiency that results from increases in aerosols [*Albrecht*, 1989]. To study both of these effects, it is desirable to use a GCM that incorporates an interactive treatment of aerosol physics and chemistry, coupled to a physically based treatment of clouds and precipitation. Calculations of these radiative effects have

been performed by *Lohmann and Feichter* [1997] and *Lohmann et al.* [2000] using versions of the European Center/Hamburg (ECHAM) model. Other studies of this type have also been performed by *Ghan et al.* [2001] and *Jones et al.* [2001]. Recently, some authors have begun to use such coupled models to explore the response of the climate system to the indirect aerosol effect [*Williams et al.*, 2001; *Rotstayn and Lohmann*, 2002].

[4] A number of GCMs now include rather complex treatments of cloud microphysics, with a substantial number of conversion terms among the prognostic variables [e.g., *Fowler et al.*, 1996; *Ghan et al.*, 1997; *Lohmann et al.*, 1999a]. These schemes have been inspired by treatments developed previously for mesoscale cloud models, and also rely on cloud-physics theory and observations. Some other cloud schemes designed for use in long GCM integrations are somewhat less complex, while still retaining the link to cloud-physics theory and observations [e.g., *Rotstayn*, 1997; *Rasch and Kristjánsson*, 1998; *Wilson and Ballard*, 1999]. On the other hand, the treatment of wet scavenging processes in global sulfur-cycle models tends to be rather simple compared to the more recent treatments of cloud microphysics in GCMs. This observation, combined with the sensitivity of sulfur-cycle models to the treatment of wet scavenging processes [*Rasch et al.*, 2000b], provides good reason to pay further attention to the treatment of this process.

[5] In this study, we describe and evaluate the simulation of the tropospheric sulfur cycle in the CSIRO GCM. The treatment of the chemistry, emissions and dry deposition is substantially based on that developed for the ECHAM3 model by *Feichter et al.* [1996], and modified for ECHAM4 as described by *Lohmann et al.* [1999a]. However, we have completely rewritten the treatment of wet scavenging, to better reflect the different properties of liquid and frozen precipitation, and the treatment of these in the model's cloud microphysical scheme [*Rotstayn*, 1997; *Rotstayn et al.*, 2000]. The new scavenging scheme is considerably more efficient than the simpler scheme used in ECHAM3 and ECHAM4.

[6] The structure of the paper is as follows. We describe the model in section 2. Results from our control run and comparisons with observations are presented in section 3. Several sensitivity tests are discussed in section 4. One of these is a run in which wet scavenging is treated by a scheme similar to that used in ECHAM, in order to gauge the impact of our scavenging scheme. Other sensitivity tests are attempts to address problems in our control run that are identified in section 3. A summary and conclusions are given in section 5.

2. Model Description

2.1. Overview of the CSIRO Atmospheric GCM

[7] The model used in this study is a low-resolution (spectral R21) version of the Mark 3 CSIRO atmospheric GCM. The CSIRO GCM is a spectral model that utilizes the flux form [*Gordon*, 1981] of the dynamical equations. Advection of water vapor, cloud water and trace quantities is handled via a semi-Lagrangian scheme (described below). The R21 model has 18 hybrid vertical levels and a horizontal resolution of approximately 5.6° longitude by 3.2° latitude. The time step is 24 min, but the leapfrog scheme

used by the model means that the time step "seen" by the model physics is 48 min.

[8] The treatments of convective and stratiform clouds and precipitation are closely coupled to the sulfur cycle, so they are briefly reviewed here. Other relevant aspects of the model's physics package are summarized by *Rotstayn* [1997].

[9] Deep convection in the model is treated using the mass-flux scheme of *Gregory and Rowntree* [1990], modified by the inclusion of downdrafts as described by *Gregory* [1995]. In common with other convection schemes used in GCMs, the convection scheme includes only a simple treatment of the microphysics of rainfall generation. Once a critical cloud depth (which differs for land and ocean points) is reached, liquid water in excess of a prescribed threshold of 0.5 g kg^{-1} falls out of the updraft. Condensate in convective updrafts is assumed to be in the liquid phase up to the $-15°C$ level, and glaciated above this level. A smaller precipitation threshold is used above the freezing level, consistent with the idea that precipitation forms more readily in ice clouds than in liquid-water clouds [e.g., *Rogers and Yau*, 1988].

[10] The stratiform cloud and precipitation scheme has been described in detail by *Rotstayn* [1997] and *Rotstayn et al.* [2000]. The scheme incorporates a simple parameterization of fractional cloudiness, prognostic variables for cloud liquid water and cloud ice, consistent treatments of warm-rain and frozen-precipitation processes, and variable cloud radiative properties. At temperatures between $-40°C$ and $0°C$, mixed-phase clouds are allowed to exist in the model [*Rotstayn et al.*, 2000]. In practice, most stratiform clouds are completely glaciated at temperatures below $-15°C$. When cloud ice and liquid water coexist in a grid box, they are assumed to exist as separate regions that are horizontally adjacent.

[11] Precipitation of cloud ice to form falling ice (loosely, snow) is parameterized via the use of an empirical fallspeed for ice particles. Precipitation of stratiform cloud liquid water occurs by autoconversion (collision and coalescence of cloud droplets), collection of cloud liquid water by raindrops, and accretion of cloud liquid water by snow. Rain and snow falling through clear air, including that in partially cloudy layers, can reevaporate. The autoconversion parameterization is sensitive to specification of the cloud-droplet number concentration, which is in turn estimated empirically from the mass concentration of sulfate following relationship D of *Boucher and Lohmann* [1995]. The cloud droplet number concentration is also used in the calculation of droplet effective radius in the radiation scheme [*Rotstayn*, 1999]. Thus, the sulfur cycle is allowed to feed back on the model's circulation, via the role of sulfate as cloud condensation nuclei (CCN). We recognize that such an empirical parameterization, in which sulfate is used as a surrogate for all aerosols that act as cloud condensation nuclei, is an oversimplification of the role of aerosols in droplet nucleation.

2.2. Treatment of the Sulfur Cycle

[12] Prognostic variables in the sulfur-cycle model are dimethyl sulfide (DMS), sulfur dioxide (SO$_2$) and sulfate. The chemistry, transport and wet and dry deposition are all calculated on-line in the GCM. The chemistry, emissions

and dry deposition are described relatively briefly, with particular reference to aspects that differ from the treatment in ECHAM4. Since we have paid considerable attention to the treatment of wet scavenging, a more detailed description of this aspect is given below.

2.2.1. Chemistry

[13] The treatment of the sulfur chemistry is very similar to that in ECHAM4 [*Feichter et al.*, 1996]. Oxidants required for the sulfur chemistry are prescribed as three-dimensional monthly mean fields. DMS and SO_2 are both oxidized by reaction with the hydroxyl (OH) radical during the day. DMS also reacts with the nitrate radical (NO_3) at night. It is assumed that the only end product of DMS oxidation is SO_2, thus ignoring the relatively small yield of methane sulfonic acid (MSA) and other oxidation products. A modification to the treatment of DMS oxidation used in ECHAM4 is introduced, following other authors who have argued that an additional (unknown) oxidant is required to obtain reasonable agreement between observed and modeled DMS concentrations [*Chin et al.*, 1996; *James et al.*, 2000]. We increase the reaction rate between DMS and OH by a factor of two, relative to the original rate given by *Hynes et al.* [1986].

[14] In the aqueous phase, SO_2 reacts with hydrogen peroxide (H_2O_2) and ozone (O_3) to form sulfate. The amount of SO_2 dissolved in cloud water is calculated according to Henry's Law. The reaction rates and the effective Henry's law constant for SO_2 are calculated assuming that aqueous phase equilibria and electroneutrality are maintained. Additionally, the simplification $[S(IV)] = [HSO_3^-]$, which can be applied if the pH ranges between 3 to 5, and the approximation of the molar ratio of sulfate to ammonium of 1 [*Dentener and Crutzen*, 1994] are used. $[H^+]$ is then approximated by:

$$[H^+] = 2[SO_4^{2-}] + [HSO_3^-] - [NH_4^+] \qquad (1)$$

Since the distribution of H_2O_2 is prescribed, the model may tend to overestimate the SO_2 oxidation rate in regions where H_2O_2 is depleted by the reaction with SO_2. On the other hand, the use of a bulk approach may underestimate in-cloud oxidation of SO_2 compared to a size-dependent model [*Roelofs*, 1993]. The aqueous-phase chemistry is applied inside the liquid-water part of stratiform clouds and inside convective clouds up to the freezing level. (Oxidation in convective clouds is not included in ECHAM4.) The convection scheme provides the vertical profile of liquid water content, but (as in other mass flux schemes) it is necessary to make an assumption about the fractional area occupied by convective cloud. This fraction is a tunable parameter of the scheme and is currently set to 0.1. This value was chosen to give a reasonable agreement between modeled and observed liquid paths in the tropics (see Figure 7) but it remains very uncertain. Note that because of the much larger liquid water contents in convective clouds compared to stratiform clouds, a larger fraction of the available SO_2 dissolves in cloud water in convective clouds. The Henry coefficients are generally less than 0.1 in stratiform clouds, but can be as large as 0.5 in convective clouds.

2.2.2. Emissions

[15] The emissions are almost identical to those used in ECHAM4 [*Lohmann et al.*, 1999a], except for the treatment of DMS emission from the ocean surface. Natural sources of sulfur in the model are SO_2 from noneruptive volcanoes, amounting to 8.0 Tg S yr^{-1} [*Spiro et al.*, 1992; *Graf et al.*, 1997], and biogenic emissions of DMS from oceans, soils and plants. Emissions of DMS from soils and plants follow *Spiro et al.* [1992] and amount to 0.9 Tg S yr^{-1}. The concentration of DMS in seawater is taken from the database of *Kettle et al.* [1999], together with the updates described by *Kettle and Andreae* [2000]. (The "raw" data are used, rather than the "assimilated" data, following advice from A. J. Kettle.) Emissions of DMS from the ocean surface are calculated using a parameterization derived by *Nightingale et al.* [2000], instead of *Liss and Merlivat* [1986] as in ECHAM4. The approach is similar to that of *Liss and Merlivat* [1986] and *Wanninkhof* [1992], except that the transfer velocity is larger than that from the former scheme and smaller than that from the latter scheme [*Kettle and Andreae*, 2000].

[16] If U_{10n} is the 10 m wind speed adjusted to neutral stability, *Nightingale et al.* [2000] propose that the transfer velocity for CO_2 at 20°C is

$$K_{CO_2} = 0.222(U_{10n})^2 + 0.333U_{10n}. \qquad (2)$$

The transfer velocity for DMS is then obtained as

$$K_{DMS} = K_{CO_2}(Sc_{DMS}/Sc_{CO_2})^{-2/3} \qquad (3)$$

for $U_{10n} < 3.6$ m s^{-1}, and

$$K_{DMS} = K_{CO_2}(Sc_{DMS}/Sc_{CO_2})^{-1/2} \qquad (4)$$

for $U_{10n} \geq 3.6$ m s^{-1}. Here, Sc_{CO2} is the Schmidt number for CO_2 at 20°C, and Sc_{DMS} is the Schmidt number for DMS, specified as a function of temperature using the cubic polynomial from *Saltzman et al.* [1993]. At grid points where sea ice exists, emission of DMS is calculated only for the areas of open water ("leads"). The model's treatment of sea ice [*O'Farrell*, 1998] allows a small fraction of open water to remain at all times. With this treatment, the annually averaged emission of DMS from the ocean surface in the control run described below is 22.1 Tg S yr^{-1}. (This is discussed in section 3.1.)

[17] Anthropogenic sources of sulfur are fossil fuel use and smelting, amounting to 66.7 Tg S yr^{-1} [*Benkovitz et al.*, 1996], and biomass burning, amounting to 2.5 Tg S yr^{-1} [*Hao et al.*, 1990]. These emissions occur as SO_2, except that 3% of the emissions from fossil fuel and smelting are assumed to occur as sulfate. (This feature is not included in ECHAM4. According to *Benkovitz et al.* [1996], between 1.4% and 5% of the total anthropogenic emissions occur as sulfate.) The anthropogenic emissions from *Benkovitz et al.* [1996] are for the year 1985, and include a substantial seasonal cycle for Europe, with winter SO_2 emissions set roughly 25% higher than the annual mean, and summer emissions set roughly 25% lower than the annual mean.

2.2.3. Transport

[18] Transport of trace quantities occurs by advection, vertical turbulent mixing and vertical transport inside deep convective clouds. Vertical advection is handled using the flux-corrected transport scheme of *Van Leer* [1977]. Horizontal advection is handled via a semi-Lagrangian scheme

[*McGregor*, 1993], which uses bicubic Lagrangian interpolation to calculate the field values at the departure points.

[19] The treatment of vertical turbulent mixing is based on stability-dependent K-theory. The diffusion coefficients are specified as functions of the Richardson number and local gradients following *Louis* [1979]. Under convective conditions, when eddies are of the same scale as the boundary layer depth, fluxes depending on local gradients are no longer valid, so an additional nonlocal countergradient flux is added, following *Holtslag and Boville* [1993].

[20] The convective transport of trace quantities is based on the vertical profiles of the updraft mass flux generated by the convection scheme. Entrainment (or detrainment) occurs in a given layer if the updraft mass flux increases (or decreases) while passing through that layer. Soluble species (sulfate and SO_2) are scavenged in updrafts as described below. DMS is insoluble, so the flux of DMS removed from below cloud base by the updraft is transported to the layer at cloud top (as well as any other layers in which detrainment occurs). In the environment outside the convective updraft, trace quantities are carried downward by compensating subsidence [e.g., *Mari et al.*, 2000].

2.2.4. Wet Scavenging

[21] The scavenging of SO_2 and sulfate by large-scale rain and snow is linked to the model's stratiform cloud scheme. In order to account for the reevaporation of SO_2 and sulfate in a manner consistent with the assumptions in the cloud scheme, it is necessary to account separately for the amounts scavenged in each layer by rain and snow. These amounts are then added to the flux of each tracer that is carried downward by rain and snow. When snow melts to form rain, the flux of tracer carried by snow is transferred to that carried by rain. Reevaporation of rain and snow are also accounted for, as described below.

[22] In-cloud (nucleation) scavenging is included for liquid-water clouds, but not for ice clouds. The sulfate inside the cloudy fraction of each grid box is assumed to be wholly dissolved in cloud droplets, though it is possible to relax this assumption, since there is observational evidence that the fraction of sulfate scavenged by cloud droplets is smaller than 1 [e.g., *Hegg et al.*, 1984]. The fraction of SO_2 dissolved in cloud droplets is given by Henry's law, as described by *Feichter et al.* [1996]. If q_l is the mixing ratio of cloud liquid water before the precipitation calculation, and the rates of autoconversion, collection by raindrops and accretion by snow are $(\dot{q}_l)_{au}$, $(\dot{q}_l)_{co}$ and $(\dot{q}_l)_{ac}$ respectively, then the fraction of in-cloud sulfate scavenged by raindrops during a time step Δt is equal to the fraction of cloud water removed as rain, namely $[(\dot{q}_l)_{au} + (\dot{q}_l)_{co}]\Delta t/q_l$. Similarly, the fraction scavenged by snow is $(\dot{q}_l)_{ac}\Delta t/q_l$. The fraction of SO_2 scavenged by raindrops is similar, but reduced by the appropriate Henry coefficient. When cloud droplets freeze due to accretion by snow, some of the dissolved SO_2 "outgases". For the fraction retained in precipitation—the so-called retention coefficient—we use the value of 0.62 found experimentally by *Iribarne et al.* [1990], although this is highly uncertain.

[23] Below-cloud scavenging is calculated using parameterizations similar to those used for the accretion processes in the stratiform cloud scheme, but with appropriate (smaller) values for the collection efficiency. These parameterizations were derived by *Rotstayn* [1997] on the assumption that
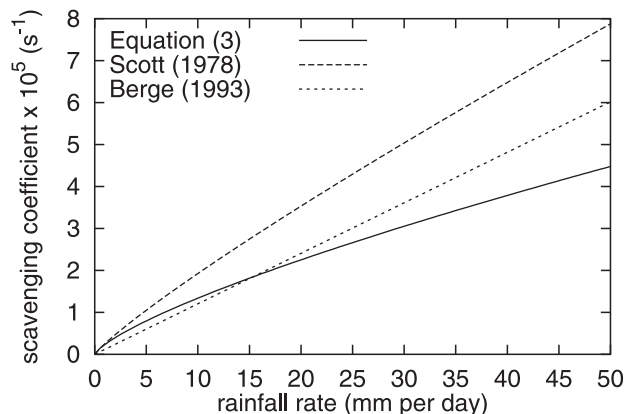
Figure 1. Scavenging coefficients when below-cloud scavenging by rain is calculated using (5), using the nonlinear form from *Scott* [1978], and using the linear approximation to Scott's scheme from *Berge* [1993]. Collection efficiency is 0.05 in (5) and 0.1 in the other two schemes. Rainfall rate is given in d^{-1}; note that (5) was expressed in $kg\ m^{-2}\ s^{-1}$.

raindrops and snowflakes follow a negative-exponential size distribution [*Marshall and Palmer*, 1948]. They are applied in the clear portion of partly cloudy grid boxes, as well as below and between cloud layers. For below-cloud scavenging by raindrops, the rate of change of mixing ratio X_i of trace species i is

$$(\dot{X}_i)_{rain} = -0.24 f_r E_i^r (R_r/f_r)^{3/4} X_i, \tag{5}$$

where f_r is the rainy fraction of the grid box, E_i^r is the collection efficiency for species i (discussed below) and R_r is the grid-box-mean rate at which rain enters the layer from above in $kg\ m^{-2}\ s^{-1}$. In (5), R_r/f_r may be regarded as the local rainfall rate, and the multiplication by f_r means that the process is applied only in the rainy fraction of the grid box. The rainy fraction is calculated assuming random overlap of cloud layers as described by *Rotstayn* [1997]; it tends to be relatively close to 1 in grid boxes with heavy stratiform rainfall (which is often associated with large cloud cover), but it can be much smaller than 1. More complex approaches can be used to calculate the rainy fraction [*Jakob and Klein*, 2000]. Fortunately, the dependence on f_r in (5) is weak, so that (for example) $f_r = 0.2$ only reduces the scavenging rate by 33% compared to $f_r = 1$.

[24] Figure 1 shows the scavenging coefficient Λ_i (defined as $-(\dot{X}_i)_{rain}/X_i$), when below-cloud scavenging is calculated using (5) with $E_i^r = 0.05$. In (5), we set $f_r = 1$ for the sake of the argument (or alternatively, the plotted scavenging coefficient can be regarded as the local value, rather than the grid-box-mean value). Then, (5) gives $\Lambda_i = 0.24\ E_i^r R_r^{0.75}$. We have also plotted the nonlinear parameterization from *Scott* [1978], and the linear approximation to Scott's scheme from *Berge* [1993]. For these two parameterizations, a fallspeed $V_r = 5\ m\ s^{-1}$ is used to express the mass concentration of raindrops (m_r) in terms of the rainfall rate ($m_r = R_r/V_r$), as suggested by *Berge* [1993]. This gives $\Lambda_i = 0.536\ E_i^r R_r^{0.875}$ for the nonlinear form, and $\Lambda_i = 1.04\ E_i^r R_r$ for the linearized form. Note that if $E_i^r = 0.1$, the linearized

Table 1. Comparison of the Wet Scavenging Schemes in the CSIRO Model (Present Scheme) and ECHAM4[a]

	CSIRO	ECHAM4
In-cloud (stratiform)	proportional to (precipitation formation rate)/ (actual LWC)	depends on (precipitation formation rate)/ (prescribed LWC) [*Giorgi and Chameides*, 1986]
In-cloud (convective)	proportional to (precipitation formation rate)/ (actual LWC)	proportional to (precipitation formation rate)/ (actual LWC)
Below-cloud	stratiform and convective	stratiform only
	nonlinear (equation (5) for rain and equation (6) for snow)	linearized (*Berge* [1993] for rain and snow)
	in partly cloudy layers	in cloud-free layers only
Reevaporation	Yes	no

[a] LWC denotes liquid water content.

form is close to the linear washout rate of 0.1 mm^{-1} that is often employed in large-scale models [*Dana and Hales*, 1976], so we have plotted Scott's and Berge's parameterizations using $E_i^r = 0.1$. It is seen that Berge's linear approximation gives lower scavenging rates than Scott's scheme, especially at low rainfall rates; it turns out that the linear approximation does not give a close match to the original scheme when quantities are expressed in SI units. (The linear approximation suggested by *Scott* [1978] was derived on the assumption that rainfall concentration was expressed in g m^{-3}.) It is also seen that, compared to the linear form that is commonly used, (5) gives larger scavenging coefficients at low rainfall rates, but smaller scavenging coefficients at high rainfall rates. Stratiform rainfall rates in the model are mostly less than 5 mm per day (even when normalized by f_r), but tropical convective rainfall rates can reach 50 mm per day in the grid-box mean. Thus, ignoring the nonlinearity may affect the balance of wet scavenging between the midlatitudes and the tropics. The treatment of convective scavenging is described below.

[25] Below-cloud scavenging by snow is calculated as

$$(\dot{X}_i)_{\text{snow}} = \frac{E_i^s \lambda_s R_s X_i}{2\rho_s}, \tag{6}$$

where E_i^s is the collection efficiency for species i, λ_s is the slope factor for the Marshall–Palmer size distribution for snow, R_s is the grid-box-mean rate at which snow enters the layer from above in kg m^{-2} s^{-1}, and ρ_s is the density of snow, taken to be 100 kg m^{-3}. λ_s is parameterized as an exponential function of temperature following *Rotstayn* [1997]. For a given flux of precipitation, (6) gives a larger scavenging rate than (5), essentially because the density of snow is a factor of 10 lower than that of rain. This means that, for a given precipitation flux, snowflakes will sweep out a larger area than raindrops. However, this is offset by the smaller collection efficiency that is applicable for snow (discussed below).

[26] The collection efficiency for aerosol particles has been reviewed by *Jylhä* [1999], who argued that for particles with diameters between 0.3 and 0.9 μm (the so-called Greenfield scavenging gap) the efficiency for collection by rain is as low as 0.02. However, we use a somewhat larger value of 0.05, as suggested by some experimental studies [e.g., *Radke et al.*, 1980], and in recognition of the fact that not all of the sulfate will exist in this size range. The average collection efficiency for aerosols by snow is generally considered to be smaller than that for rain, and we adopt the value of 0.01 suggested by *Jylhä* [1999]. In reality, the collection efficiency

is a strong function of aerosol size, so the use of a single bulk collection efficiency is a simplification.

[27] Estimation of the collection efficiency for a moderately soluble gas such as SO_2 is complex [*Pruppacher and Klett*, 1997; *Seinfeld and Pandis*, 1998], and different approximations have been suggested for use in large-scale models. A possible approach [e.g., *Berge*, 1993] is to use Henry's law, although for the larger raindrops the equilibrium assumption may overestimate the scavenging rate [*Easter and Luecken*, 1988]. In view of this uncertainty, we specify a collection efficiency of 0.05 for SO_2, the same value as used for sulfate. Experimental studies reviewed by *Pruppacher and Klett* [1997] give a range of 5×10^{-6} to 6×10^{-5} s^{-1} for the scavenging coefficient of SO_2 by rain. Using (5) with $E_i^r = 0.05$, these lower and upper limits are obtained with local rainfall rates of 2.7 mm per day (3.1×10^{-5} kg m^{-2} s^{-1}) and 74 mm per day (8.6×10^{-4} kg m^{-2} s^{-1}) respectively, as shown in Figure 1. Thus, the collection efficiency of 0.05 seems plausible, though very uncertain.

[28] Experimental studies reviewed by *Pruppacher and Klett* [1997] indicate that SO_2 can be adsorbed onto the surface of ice particles, especially at temperatures close to 0°C, but no theoretical formulations currently exist for the rate of adsorption. Based on laboratory studies, *Diehl et al.* [1998] showed that under atmospheric conditions the direct uptake of SO_2 by ice particles is small compared to the uptake by water drops. We therefore omit below-cloud scavenging of SO_2 by snow in the standard version of our scheme.

[29] The rates of reevaporation of large-scale rain and snow are calculated using parameterizations derived by *Rotstayn* [1997]. The fraction of scavenged SO_2 that reevaporates is set equal to the fraction of rain or snow that reevaporates. Applying this assumption to the reevaporation of raindrops containing sulfate is likely to overestimate the rate of reevaporation of sulfate, since the number of raindrops that completely evaporate and liberate an aerosol particle is less than proportional to the mass of rain that evaporates. Following *Koch et al.* [1999], we set the fraction of sulfate that reevaporates equal to an arbitrary 50% of the fraction of rain that reevaporates.

[30] In deep convective updrafts, sulfate and SO_2 are scavenged by an analogous method, bearing in mind that convective precipitation formation is treated by a simple threshold scheme as described above. Thus, sulfate in updrafts is scavenged in direct proportion to the fraction of liquid water that precipitates out of the updraft at a given level, and SO_2 is scavenged in a similar manner, but reduced by the appropriate Henry coefficient. Above the

freezing level ($-15°C$), scavenging in updrafts is assumed to be zero. Below convective cloud base, and in air outside convective cloud that is not occupied by large-scale liquid-water cloud, below-cloud scavenging by convective precipitation is included according to (5), with $f_r = 0.3$. Use of (5) entails the simplifying assumption that all convective precipitation occurs as rain. Below convective cloud base, reevaporation of sulfate and SO_2 occurs following an analogous method to that described above for large-scale rain.

[31] Table 1 contains a summary of the main differences between the present treatment of wet scavenging, and that used in ECHAM4. As we show in section 4 the net effect of these differences is that the present scheme gives generally larger scavenging rates and a smaller global sulfate burden. The most crucial differences concern the below-cloud scavenging, because in addition to using a less efficient parameterization, the ECHAM4 scheme does not allow it to occur in the clear portion of partly cloudy layers, or below convective clouds.

2.2.5. Dry Deposition

[32] The treatment of dry deposition is essentially the same as that used in ECHAM4 [*Lohmann et al.*, 1999a]. The dry deposition flux to the surface is assumed to be proportional to the product of the concentration in the lowest model level (about 35 m above the surface) and a prescribed dry deposition velocity [*Ganzeveld et al.*, 1998]. For sulfate, this is assumed to be 0.025 cm s^{-1} over dry surfaces and 0.2 cm s^{-1} over wetted surfaces (including vegetation, and melting snow and ice). For SO_2, it is assumed to be 0.1 cm s^{-1} over nonmelting snow and ice, 0.2 cm s^{-1} over dry soil, and 0.8 cm s^{-1} over wetted surfaces. For partially wet soil, it is scaled between the applicable dry and wet values as a linear function of the soil moisture.

2.2.6. Summary of Main Differences From the Sulfur Cycle in ECHAM4

[33] The most substantial differences relative to ECHAM4 concern the wet scavenging, as summarized in Table 1. Our treatment of DMS emission from the ocean surface uses a flux parameterization [*Nightingale et al.*, 2000] that gives larger fluxes than the scheme of *Liss and Merlivat* [1986] used in ECHAM4. We also updated the database of DMS in seawater to the most recent one available [*Kettle et al.*, 1999]. Changes to the chemistry are the increase of the oxidation rate of DMS, and the inclusion of aqueous oxidation of SO_2 in convective clouds. Transport in our scheme is calculated by methods intrinsic to the CSIRO model, so these differ from those in ECHAM4. In particular, while both models use mass-flux convection schemes, we have calculated the convective transport in an "offline" manner, using mass fluxes saved from the convection scheme. In contrast, ECHAM4 calculates convective transport during the call to the *Tiedtke* [1993] convection scheme.

3. Control Simulation: Results and Comparison With Observations

[34] In this section, we focus on a run performed with the model described above, hereafter referred to as the CONTROL run. The model was initialized from a state corresponding to 1 November from a run performed with a slightly

Table 2. Annual Average Global Sulfur Budgets for Years 4–8 of the CONTROL Run (This Work) and ECHAM4

	This Work	ECHAM4[a]	Other Models[b]
DMS			
Source: emission	22.1	19.0	10.7–23.7
Sink: oxidation	22.1	19.0	10.7–23.7
Burden	0.085	0.15	0.020–0.13
Lifetime	1.4	2.9	0.5–3.0
SO₂			
Sources: emission	75.2 (77%)	77.3 (80%)	64.8–104.0
DMS oxidation	22.1 (23%)	19.0 (20%)	10.0–24.7
Sinks: dry deposition	33.6 (35%)	36.6 (38%)	16.0–55.0
wet deposition	7.5 (8%)	4.8 (5%)	0.0–19.9
gas-phase oxidation	10.2 (10%)	12.5 (13%)	6.1–16.2
aqueous oxidation	45.9 (47%)	42.4 (44%)	24.5–57.8
Burden	0.42	0.54	0.20–0.61
Lifetime	1.6	2.0	0.6–2.6
Sulfate			
Sources: emission	2.0 (3%)	0	0–3.5
SO₂ oxidation	56.1 (97%)	54.9 (100%)	44.7–74.7
Sinks: dry deposition	7.2 (12%)	8.8 (16%)	3.9–18.0
wet deposition	50.8(88%)	46.1 (84%)	34.7–61.0
Burden	0.67	1.05	0.53–0.96
Lifetime	4.2	6.9	3.9–5.8

Sources and sinks are expressed in Tg S yr^{-1}, burdens in Tg S, and lifetimes in days.
[a]From *Lohmann and Feichter* [1997] and *Lohmann et al.* [1999b].
[b]Range of results from *Langner and Rodhe* [1991], *Pham et al.* [1995], *Chin et al.* [1996], *Feichter et al.* [1996], *Chuang et al.* [1997], *Lelieveld et al.* [1997], *Roelofs et al.* [1998], *Koch et al.* [1999], *Rasch et al.* [2000a], and *Chin et al.* [2000a].

different version of the model. It was integrated for two months, and then for a further eight years, for which period the model statistics were saved as monthly means. The two-month spinup is sufficient for results at the surface, but may be insufficient for the stratosphere or upper troposphere. We therefore show comparisons with surface observations for the entire eight-year period (to minimize the impact of interannual variability), but use only Years 4–8 for other results from the model. Concentrations of trace quantities are shown in parts per trillion by mole (ppt) or parts per billion by mole (ppb).

3.1. Global Results

[35] The global sulfur budget from Years 4–8 of our CONTROL run is summarized in Table 2, together with results from ECHAM4 and a range of results from other global models. The version of ECHAM4 we refer to [*Lohmann and Feichter*, 1997; *Lohmann et al.*, 1999b] is the most recent for which a global sulfur budget has been published. Note that ECHAM4 has a much larger global sulfate burden than ECHAM3, which was described by *Feichter et al.* [1996]. This change in ECHAM occurred with the introduction of the autoconversion scheme from *Beheng* [1994], which is strongly dependent on cloud droplet concentration. A strong positive feedback between sulfate mass and droplet concentration resulted in a decrease in precipitation and wet scavenging, and an increase in the liquid-water path and sulfate burden. (Results given by *Lohmann et al.* [1999a] show that the liquid-water path over oceans in ECHAM4 is indeed larger than satellite-retrieved values.) In ECHAM3, autoconversion was parameterized following *Sundqvist* [1978], and did not depend on droplet concentration. Liquid-water paths from our

CONTROL run are compared with satellite-retrieved values in section 3.2.1.

[36] Our global emission of DMS (22.1 Tg S yr^{-1}) is well within the range of 15 to 33 Tg S yr^{-1} suggested by *Kettle and Andreae* [2000], but is toward the high end of values obtained in other global models. Our larger emission of DMS compared to ECHAM4 is due to the use of the parameterization from *Nightingale et al.* [2000] instead of *Liss and Merlivat* [1986]. However, the difference is smaller than one would expect from a comparison of these two parameterizations (see section 4). The database for the concentration of DMS in seawater used in this version of ECHAM [*Bates et al.*, 1987] gives larger concentrations overall than those given by *Kettle et al.* [1999], and this partially compensates for the less efficient flux parameterization in ECHAM4.

[37] The burdens of DMS, SO$_2$ and sulfate in the CSIRO model are not especially large or small compared to the range of results from other global models. On the other hand, ECHAM4 has relatively large burdens of DMS and sulfate compared to other models. Our DMS burden is lower than that in ECHAM4, despite a larger emission of DMS. This is because of the enhanced rate of oxidation of DMS in our model (see section 4). The smaller sulfate burden in our model is mostly related to the more efficient treatment of wet scavenging; this is considered further in section 4. The total rate of aqueous oxidation of SO$_2$ is similar in the two models, but a result not given in Table 2 is that the fraction of aqueous oxidation by O$_3$ is smaller in ECHAM4 (7%) than in our model (19%). This is because of the higher sulfate burden in ECHAM4, giving more acidic cloud water, and our inclusion of oxidation of SO$_2$ in convective clouds, which have larger liquid water contents and hence lower acidity than stratiform clouds. In other respects, the global budgets from the two models are not remarkably different.

[38] Our value for wet deposition of SO$_2$ (7.5 Tg S yr^{-1}) lies roughly in the middle of a large range of values from other models. As discussed by *Rasch et al.* [2000a] and other authors, the large range of values is in part a labeling issue, since it depends on whether SO$_2$ oxidized in cloud water and then scavenged is counted as SO$_2$ or sulfate. We count it as sulfate, so our value for wet deposition of SO$_2$ represents SO$_2$ scavenged in cloud water by Henry's Law but not oxidized, plus below-cloud scavenging of SO$_2$. The largest contribution in our model is from below-cloud scavenging, and this depends on a very uncertain collection efficiency of 0.05. Note that we do not calculate aqueous oxidation of SO$_2$ in falling rain, so our value does not exactly represent the wet deposition of S(IV) as opposed to S(VI). The fraction of wet deposition that occurs as S(IV) is itself very uncertain [*Wojcik and Chang*, 1997], so the large range of model results is not entirely a labeling issue.

[39] Figure 2 shows the modeled column burdens of DMS, SO$_2$ and sulfate for December to February (DJF) and June to August (JJA). The largest burdens of DMS occur over the Southern Ocean in DJF. As expected, SO$_2$ and sulfate burdens are largest over the industrialized areas, and there are weaker maxima associated with biomass burning in the tropics. Over the industrialized areas of the Northern Hemisphere, SO$_2$ burdens are larger during winter, whereas sulfate burdens are larger during summer.

[40] A zonally averaged view of the modeled DMS, SO$_2$ and sulfate is presented in Figure 3. These results can be compared, for example, with those presented for the GOCART model by *Chin et al.* [2000a], as well as those of other authors. (The GOCART model is driven by analyzed meteorology, thus reducing errors associated with the meteorology that drives the sulfur cycle. There is still considerable uncertainty related to the treatment of the sulfur cycle itself.) The distribution of DMS is similar to that shown by *Chin et al.*, and the maximum in the upper troposphere due to vertical transport by deep convection is a noticeable feature. Some of the observations from field experiments presented by *Chin et al.* [1996, 2000b] do show evidence of such an enhancement in the tropical upper troposphere. The distributions of SO$_2$ and sulfate show regions of depletion in the middle to upper tropical troposphere. These features are again similar to those from the GOCART model, and are due to the efficient scavenging of SO$_2$ and sulfate in convective updrafts. In our model, the depletion of SO$_2$ in the tropical troposphere is quite strong, whereas the depletion of sulfate is noticeably weaker than in the GOCART model. This is in part because of our inclusion of oxidation of SO$_2$ in convective clouds. (In section 4 we briefly consider a run without this process). As noted by *Chin et al.* [2000a], some other global simulations have shown this depletion [e.g., *Feichter et al.*, 1996; *Koch et al.*, 1999], whereas others have not [e.g., *Chin et al.*, 1996; *Barth et al.*, 2000]. It is unclear which of the models are the more realistic. Another aspect of the SO$_2$ and sulfate distributions from our model is that the concentrations at middle to high latitudes of the Southern Hemisphere are relatively large (e.g., compared to those from the GOCART model). This is due to the larger values of DMS emission, combined with efficient oxidation of DMS, which causes the effect of the DMS emission to be seen more strongly in the SO$_2$ and sulfate distributions than in the DMS distribution.

3.2. Comparison With Observations
3.2.1. Overview

[41] In this subsection, we make substantial use of surface observations of SO$_2$, sulfate and wet deposition of sulfate corrected for sea salt from the Eulerian Model Evaluation Field Study (EMEFS) over North America [*McNaughton and Vet*, 1996], and the Cooperative Program for Monitoring and Evaluation of the Long Range Transmission of Air Pollutants in Europe (EMEP) [*Schaug et al.*, 1987]. The EMEFS data used in this study cover the period from July 1988 to May 1990, and were processed as described by *Kasibhatla et al.* [1997]. The region covered by these data is predominantly in eastern North America, and has been shown by *Kasibhatla et al.* [1997] and *Barth et al.* [2000]. The EMEP data are chosen to cover the period 1982–1988 (rather than 1983–1992 as in the work of *Kasibhatla et al.* [1997]) to minimize any bias over Europe due to trends in the emissions. We eliminated stations west of 15°W (Iceland) or north of 70°N, in order to focus on a relatively compact area covering continental Europe, Britain and Ireland. We further eliminated stations located more than 600 m above sea level (because the model does not resolve steep topography), or for which there were not at least three full years of data during the seven-year period, and then calculated monthly means at each station. This
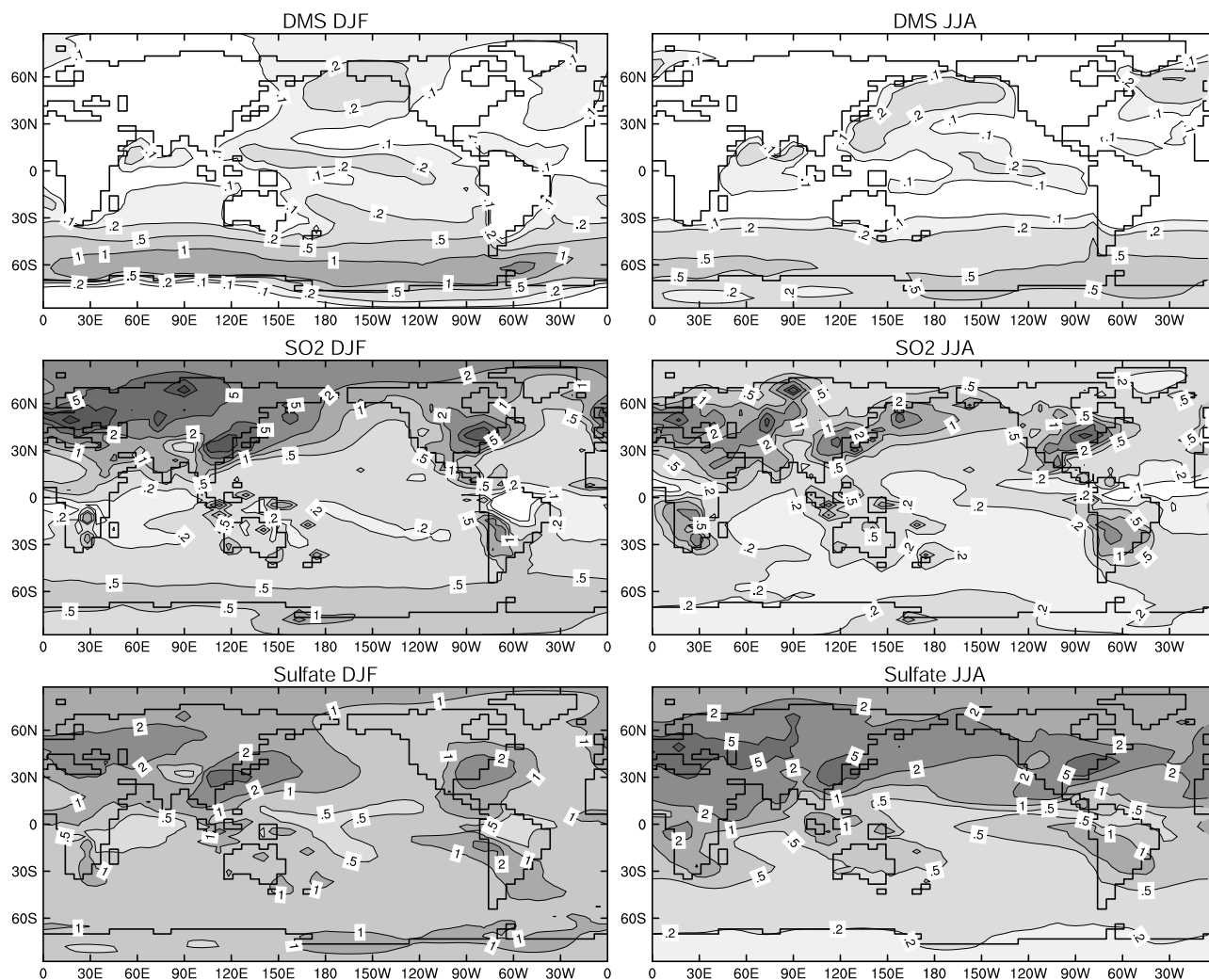
Figure 2. Column burdens of DMS, SO_2, and sulfate for December to February (DJF) and June to August (JJA) for Years 4–8 of the CONTROL run. Contours are 0.1, 0.2, 0.5, 1, 2, 5, 10, 20 mg S m^{-2}.

gave 52 stations for the wet deposition data, and 55 for SO_2 and sulfate. We then assigned each station to a grid box from the R21 model, and used the data on the model grid to compute averages over these regions. The areas on the model grid corresponding to the EMEP observations for SO_2, sulfate, and wet deposition of sulfur are shown in Figure 4. It can be seen that the three sets of grid points are similar, but not identical. For each quantity, we have used the entire set of applicable grid points, rather than restricting the comparison to the intersection of the three sets. Some data from selected single stations are used for comparison of observed and modeled annual cycles. We also use observations of DMS, SO_2 and non-sea-salt (nss) sulfate at a number of remote sites; details of these are given below.

[42] Table 3 summarizes annual-mean surface data from the model and observations, averaged over two "polluted" regions and two "remote" regions. For Europe and North America, we averaged the model output and observations over all the grid boxes covered by the EMEP and EMEFS networks (described above). For sulfate and wet deposition of sulfur in the oceanic and Antarctic regions, we averaged the model output and observations over the limited set of points for which we had long-term observations (as listed in

Table 3). For SO_2, we only had limited observations from field experiments, so we averaged the model output over broader areas as indicated in Table 3. The model agrees better with the observations over Europe than over North America, where it shows a positive bias in all quantities. Over oceanic points in the Southern Hemisphere (SH), the model is in reasonable agreement with the observations, bearing in mind the limited number of data points. At Antarctic points, the modeled sulfate concentration is almost twice the observed value, while the wet deposition at the South Pole is smaller than that observed, suggesting that the model underestimates wet deposition in this region. Few observations of Antarctic SO_2 are available, but comparison with the observed value for March–April 1986 from *Berresheim* [1987] suggests that the modeled SO_2 is also too large in the Antarctic and sub-Antarctic region. The simulation in that region is highly sensitive to the treatment of DMS emission from the ocean surface; we show in section 4 that better results are obtained there using a different parameterization of the DMS flux.

[43] The scatterplots of modeled versus observed quantities for the North American (EMEFS) region in Figure 5 give an overview of the results there. The summer results
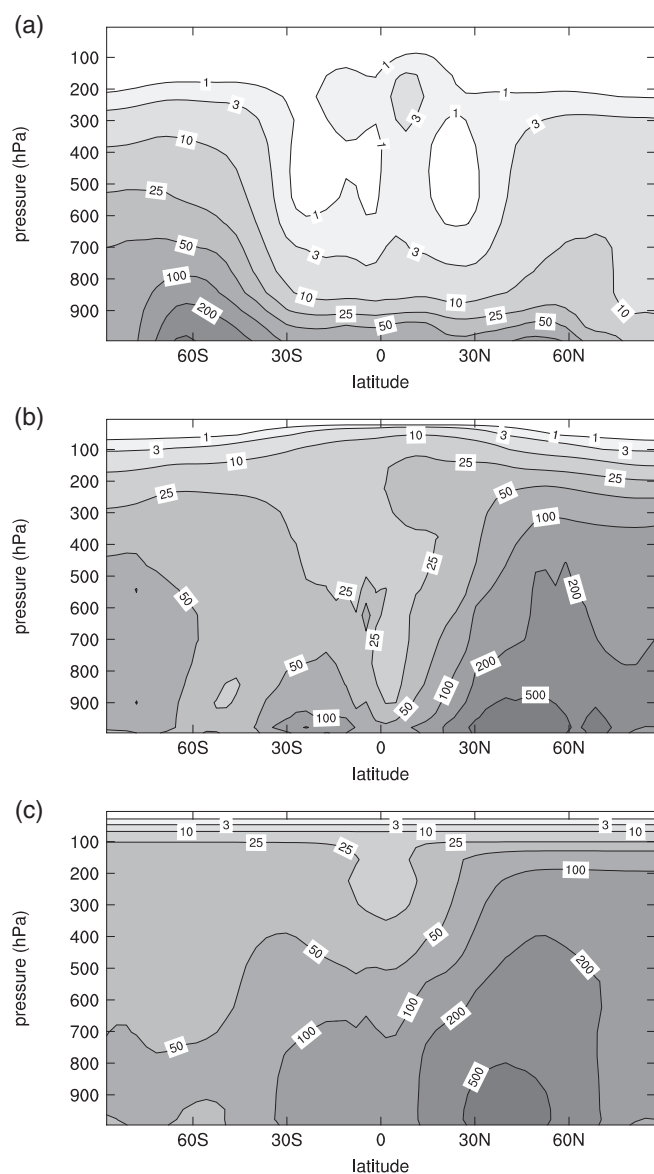
Figure 3. Annually and zonally averaged distribution of (a) DMS, (b) SO_2, and (c) sulfate for Years 4–8 of the CONTROL run. Contours are 1, 3, 10, 25, 50, 100, 200, 500 ppt.

Table 3. Annual Mean Modeled SO_2, Sulfate, and Wet Deposition of Sulfur at the Surface for Selected Regions, With Observed Values in Parentheses

Experiment	SO_2	Sulfate	Wet Deposition
Europe	3193 (3161)[a]	1254 (1259)[a]	805 (882)[a]
North America	3479 (2060)[b]	1265 (1073)[b]	663 (610)[b]
SH oceanic	42 (16−71)[c]	82 (74)[d]	58 (77)[e]
Antarctic	30 (11)[f]	49 (25)[g]	0.14 (1)[h]

SO_2 and sulfate concentrations are expressed in ppt and wet deposition in mg S m^{-2} yr^{-1}.

[a] From EMEP for 1982–1988 (see text and Figure 4 for details).

[b] From EMEFS for 1988–1990 (see text and *Barth et al.* [2000] for details). Wet deposition annual means estimated from the average of summer and winter values.

[c] Range of observed values over SH oceans summarized by *Langner and Rodhe* [1991] and *Chin et al.* [1996]. Modeled value is annual mean over oceanic points equatorward of 60°S.

[d] American Samoa, New Caledonia, Norfolk Island, Cape Grim, Chatham Island, Prince Edward Island, and Reunion Island [from *Chin et al.*, 1996; from D. L. Savoie and J. M. Prospero, unpublished data].

[e] American Samoa, Amsterdam Island, central Tasman Sea, and Macquarie Island [from *Chin et al.*, 1996, and references therein].

[f] Observations for March–April 1986 between 55°S and 65°S from *Berresheim* [1987]. Modeled value averaged over that region for March and April.

[g] Mawson, Palmer, and South Pole [*Savoie et al.*, 1993; *Tuncel et al.*, 1989].

[h] South Pole [*Legrand and Delmas*, 1984].

are in overall better agreement with the observations than the winter results. In winter, SO_2 and sulfate at a substantial number of points differ by more than a factor of two from the observations, and the slope in the data is suggestive of a lack of transport away from the major source region. In particular, the winter sulfate plot shows a small total variation in the observations, and a tendency for the model sulfate to be too high (low) in the more (less) polluted areas. This pattern was a feature of most of the models compared by *Rasch et al.* [2000b], and is also evident in the recent results of *Chin et al.* [2000b] in a model driven by analyzed meteorology. In summer, the modeled sulfate tends to be somewhat lower than observed, whereas the SO_2 tends to be somewhat higher than observed in the more polluted areas. Comparison of the modeled cloudiness with observations from the International Satellite Cloud Climatology Project [*Rossow et al.*, 1996] shows that the model has deficient cloud cover over the continental US in summer, so a lack of oxidation in clouds is a possible reason for this. The model correctly captures the tendency for wet deposition to be
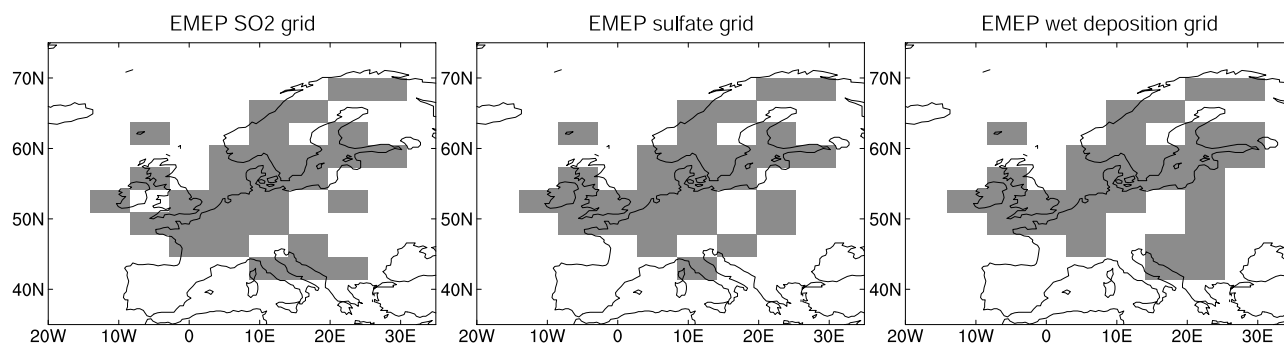
Figure 4. Map showing the model grid points corresponding to the network of EMEP observations for SO_2, sulfate and wet deposition of sulfur for the period 1982–1988.
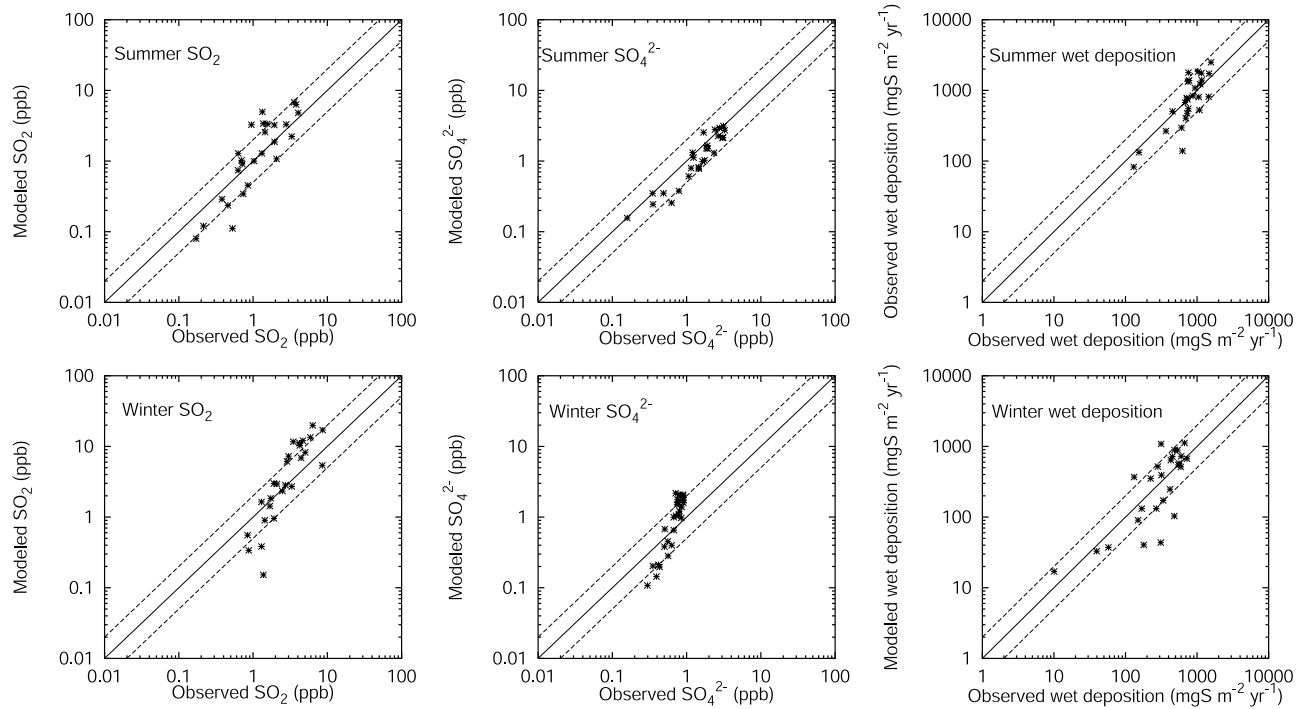
Figure 5. Observed versus modeled SO_2, sulfate and wet deposition of sulfur at the surface for summer (JJA) and winter (DJF) in North America. The 1:1 lines (solid) and the 1:2 and 2:1 lines (dashed) are shown for reference.

higher in summer than winter, although there is again a tendency for the modeled values to be too high (low) in the more (less) polluted areas.

[44] In Europe (Figure 6) the model mostly agrees with the observations to within a factor of two. There is a low bias in the modeled sulfate concentrations during winter. This is a typical finding, and according to *Chin et al.* [2000b], it is likely to be because of the sea-salt component in the EMEP data, which is largest in winter. In summer there is a mild tendency for the model to show high (low) sulfate concentrations in the more (less) polluted areas. In both North America and Europe, wet deposition tends to be
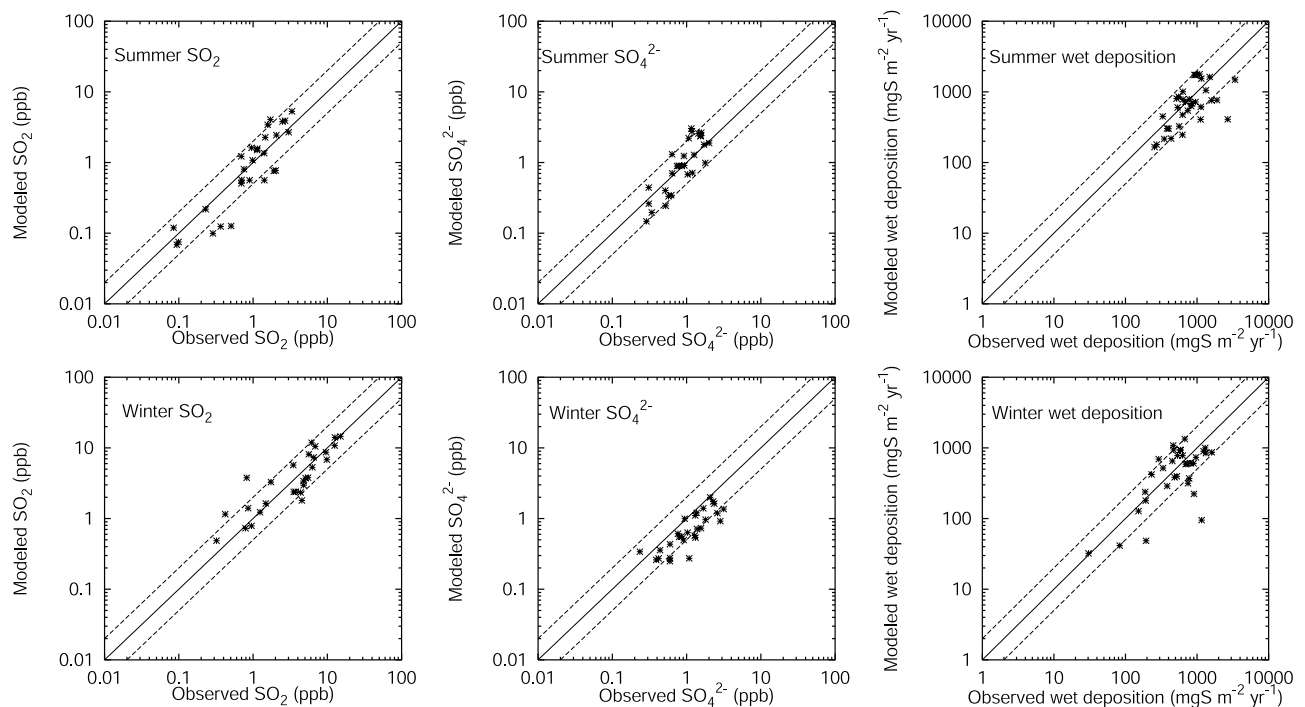
Figure 6. Observed versus modeled SO_2, sulfate and wet deposition of sulfur at the surface for summer (JJA) and winter (DJF) in Europe. The 1:1 lines (solid) and the 1:2 and 2:1 lines (dashed) are shown for reference.
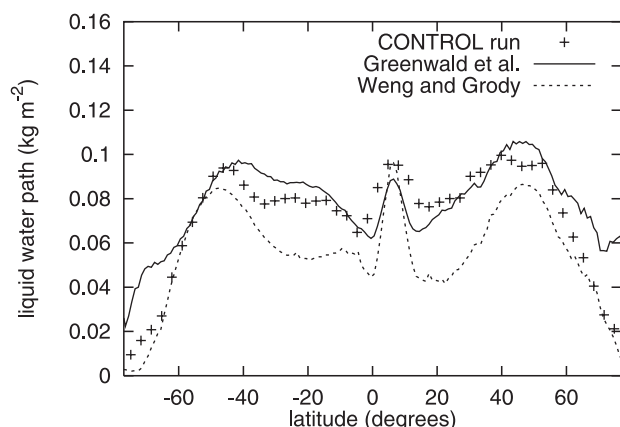
Figure 7. Modeled and satellite-retrieved liquid-water paths, zonally averaged over oceans. Satellite-retrieved values are from *Greenwald et al.* [1993] and *Weng and Grody* [1994].

in reasonable agreement with the observations, though there are a few points where the modeled wet deposition is much too low. These are mainly associated with low modeled sulfate concentrations in the model.

[45] We described in section 3.1. how the introduction of a new autoconversion parameterization in ECHAM4 resulted in a large increase in the sulfate burden, due to a reduction in precipitation and increase in liquid-water path in polluted areas. The distribution of liquid water in a climate model depends on many factors, including the link

between the sulfate distribution and the autoconversion process. In the CSIRO model, this link occurs through the parameterization of droplet concentration as a function of sulfate mass [*Boucher and Lohmann*, 1995] and through the dependence of autoconversion on droplet concentration [*Tripoli and Cotton*, 1980]. Both of these parameterizations are highly simplified representations of complex processes. As a first step, the modeled liquid-water paths can be compared with satellite-retrieved values (although these are only available over oceans). Figure 7 compares the zonally averaged liquid-water paths over oceans from the CONTROL run and from the satellite retrievals of *Greenwald et al.* [1993] and *Weng and Grody* [1994]. There are large differences between the two satellite retrievals, and the model tends to agree better with the first retrieval. This result suggests that the model does not seriously misrepresent the liquid-water paths over oceans, but clearly there is a need to reduce the uncertainty in the observations.

3.2.2. Seasonal Cycles

[46] Further insight into the above results is achieved by comparison of the seasonal cycles of modeled and observed surface concentrations at selected points. With the exception of the point denoted "central-eastern Germany" (described below), all observations are from a single site, and are compared with the model output from the single grid box that contains that site.

[47] Long-term observations of DMS are available at Amsterdam Island [*Sciare et al.*, 2000] and Cape Grim [*Ayers et al.*, 1995]. Figure 8 shows the seasonal cycle of modeled and observed surface concentrations of DMS at
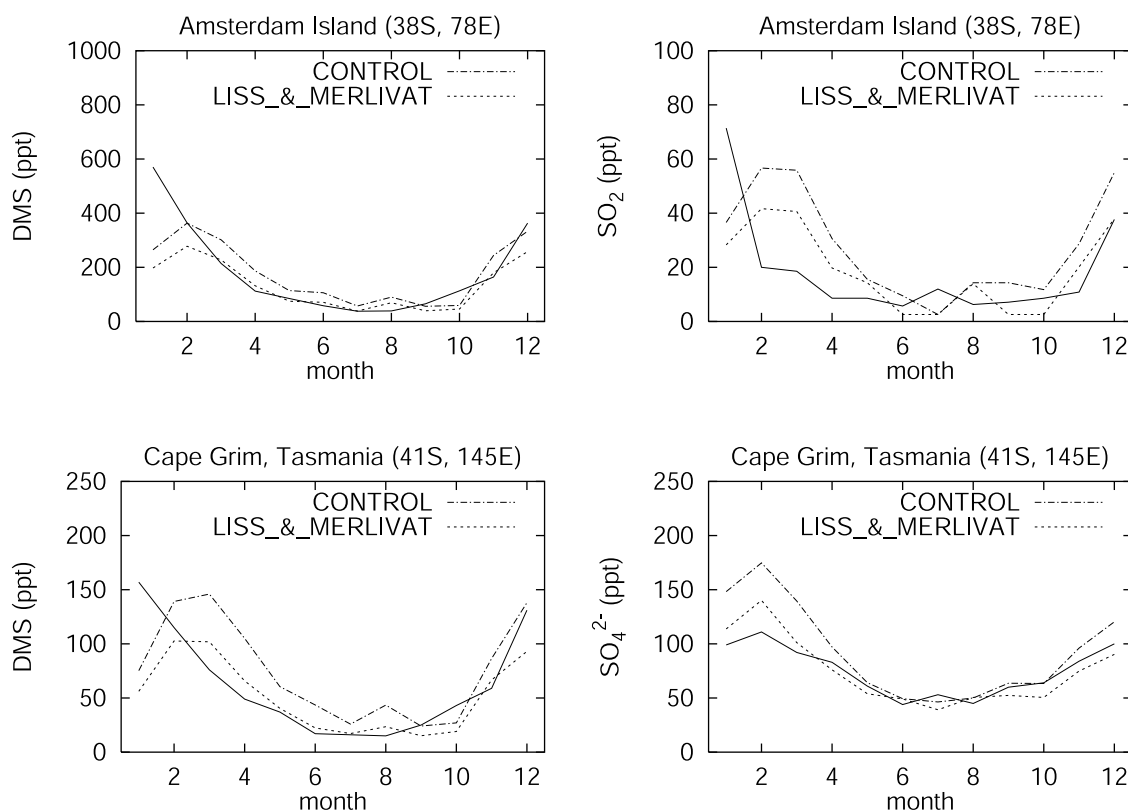
Figure 8. Seasonal variation of observed (solid lines) and modeled (dashed lines) monthly mean surface concentrations of DMS at Amsterdam Island and Cape Grim, SO_2 at Amsterdam Island and nss-sulfate at Cape Grim. Results are also shown for the LISS_&_MERLIVAT run, described in section 4.
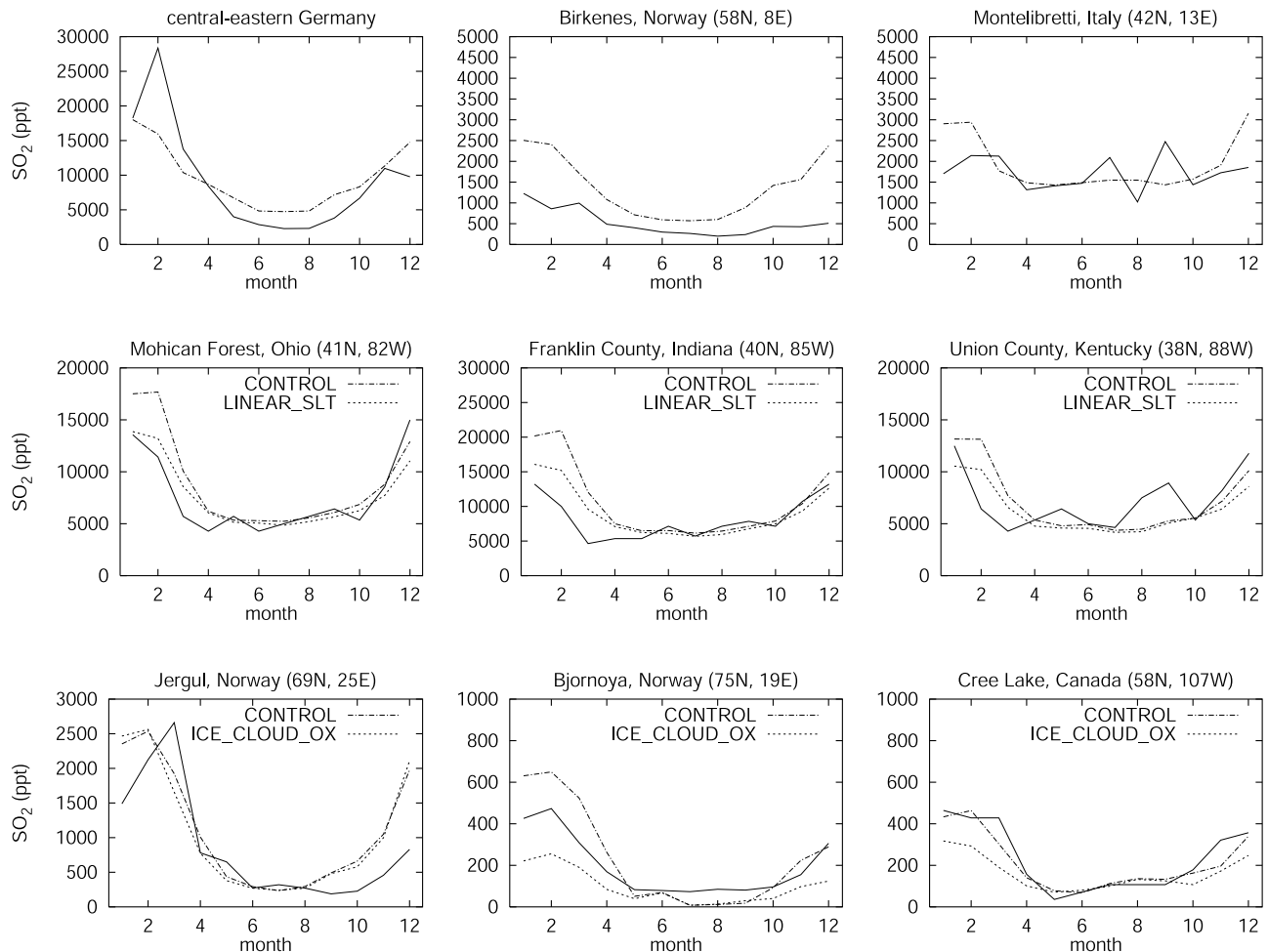
Figure 9. Seasonal variation of observed (solid lines) and modeled (dashed lines) monthly mean surface concentrations of SO_2. Observations are from EMEP for European sites and from *Chin et al.* [1996] and references therein for North American sites. For selected sites, results are also shown for the LINEAR_SLT and ICE_CLOUD_OX runs, described in section 4. The area denoted as "central-eastern Germany" is described in the text.

these sites, together with SO_2 at Amsterdam Island [*Nguyen et al.*, 1992] and nss-sulfate at Cape Grim (D. L. Savoie and J. M. Prospero, unpublished data, 1983–1996). The SO_2 observations at Amsterdam Island span slightly less than two years, so interannual variability may be a limiting factor in the interpretation of these. The model is broadly able to capture the observed seasonal cycles at both sites. The mean modeled DMS values at Cape Grim appear to be too large, whereas the mean modeled values at Amsterdam Island are in better agreement with the observations. At both sites, the maxima in the model occur in February or March, a little later than the observed maxima. A contributing factor to this discrepancy appears to be the month-to-month variations in the climatological seawater DMS concentrations from *Kettle et al.* [1999], which are markedly lower at both points in January than in February. The modeled SO_2 at Amsterdam Island and sulfate at Cape Grim agree better with the observations in winter than in summer, when the modeled values tend to be too large. In section 4, we consider results from the LISS_&_MERLIVAT run, in which DMS emission from the ocean surface is calculated using the scheme of *Liss and Merlivat* [1986].

[48] Figure 9 shows the seasonal cycle of modeled and observed SO_2 at three sites in Europe, three in the USA and three at Arctic or sub-Arctic sites. (In central Europe, topographic effects can result in large differences in the observations at stations within a single model grid box, so we averaged the data from four EMEP stations that lie within the grid box centered at 49.38°N, 11.25°E to obtain the observed seasonal cycle corresponding to this grid box, which we denote "central-eastern Germany". The four stations are at Usingen, Ansbach, Rottenburg and Hof.) The seasonal cycle of SO_2 is broadly captured by the model in each region, but there are marked differences between regions in the quality of the simulation. In Europe, the seasonal cycle is underestimated at the grid box corresponding to central-eastern Germany. At Birkenes in Northern Europe, the modeled SO_2 is too high throughout the year, whereas at Montelibretti in Southern Europe, the simulation is relatively good. In the US, the model tends to show good agreement with the observations in summer, and somewhat higher values than the observations in winter. At Jergul and Bjørnøya (Bear Island), the model tends to show excessive levels of SO_2 in winter, in common with a number of other
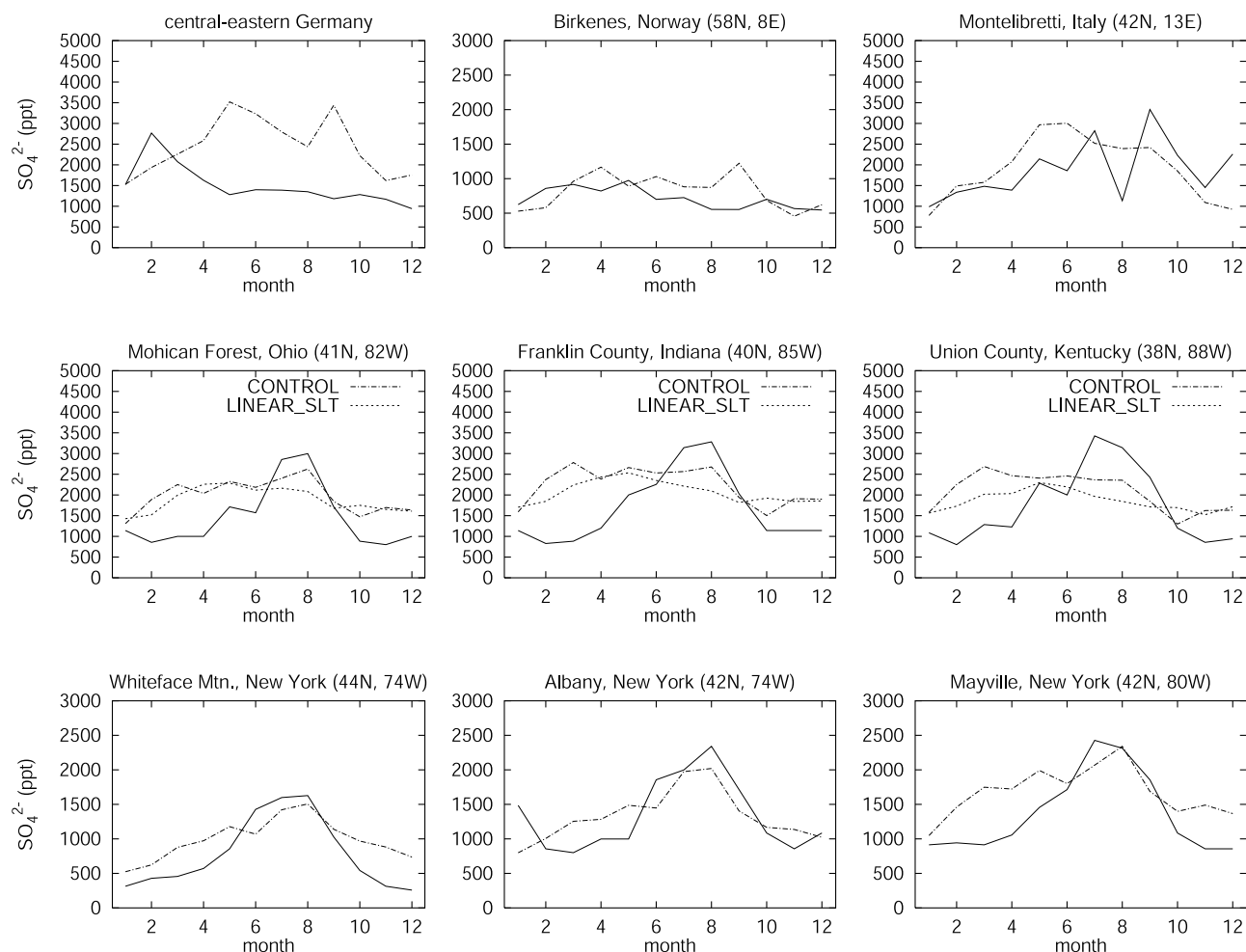
Figure 10. Seasonal variation of observed (solid lines) and modeled (dashed lines) monthly mean surface concentrations of sulfate at European and North American sites. Observations are from EMEP for European sites and from *Chin et al.* [1996] and references therein for North American sites. For North American sites, results are also shown for the LINEAR_SLT run, described in section 4. The area denoted as "central-eastern Germany" is described in the text.

recent models [e.g., *Chin et al.*, 1996; *Barth et al.*, 2000]. In section 4, we consider two sensitivity tests that pertain to this problem: the EUROPE_CYCLE run, in which we increase the seasonal cycle of European SO_2 emissions, and the ICE_CLOUD_OX run, in which we allow oxidation of SO_2 to occur in ice clouds.

[49] The seasonal cycles of surface sulfate concentration for the European and American sites considered above are shown in Figure 10, along with results for three additional sites in the US. In central-eastern Germany and to a lesser extent at Birkenes, the modeled sulfate is too large, except during winter. Combined with the similar finding for SO_2, this is consistent with the suggestion of *Chin et al.* [2000b] that either the emission rates are too high, or there is an additional loss of SO_2 that does not lead to a significant sulfate production. One possibility is that the model is not transporting trace quantities away from the source area sufficiently quickly. Better agreement between the model and observations is again obtained at Montelibretti in Southern Europe. In the US, the three points in the Midwest all show a similar pattern of excessive modeled sulfate in winter. The modeled wet deposition of sulfur for DJF,

averaged over the EMEFS network, is 352 mg S m^{-2} yr^{-1}, only slightly less than the observed value (370 mg S m^{-2} yr^{-1}). This suggests that a lack of wet deposition in winter is not the cause of the problem. Since the SO_2 values there were also too high, a possible explanation is a lack of transport away from the source area. In section 4, we consider a sensitivity test (LINEAR_SLT) in which a different horizontal advection scheme is used, and show that there is some improvement in this region. Compared to the sites in the Midwest, the three sites in New York show better agreement between the modeled and observed sulfate concentrations.

[50] A simplified view of the European results is presented in Figure 11, in which the data have been averaged over the region covered by the EMEP network. The first plot confirms that the model broadly captures the seasonal cycle of SO_2 over Europe, although the magnitude of the seasonal cycle is somewhat underestimated and the modeled SO_2 peaks earlier than the observed. This suggests that the simulation could benefit from SO_2 emissions that peak in February (instead of emissions that are "flat" for each of the four seasons), and also from a larger seasonal cycle in the
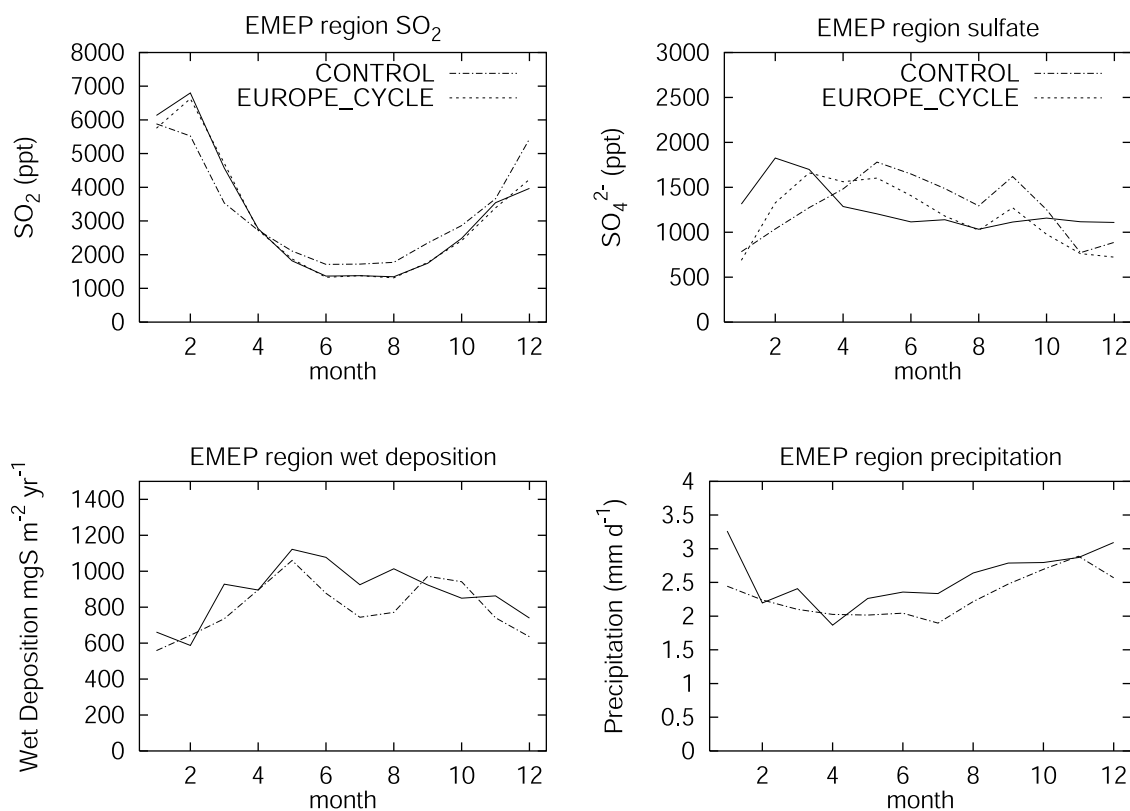
Figure 11. Seasonal variation of observed (solid lines) and modeled (dashed lines) monthly mean SO_2, sulfate, wet deposition of sulfur and precipitation for the region covered by the EMEP network in Europe. Precipitation observations are for 1982–1988 from the Global Precipitation Climatology Project (GPCP) Version 2 *Huffman et al.* [1997]. SO_2 and sulfate are also shown for the EUROPE_CYCLE run, described in section 4.

SO_2 emissions. The model underestimates the sulfate concentration in winter, and overestimates it in summer, so the error in the sulfate is in the same direction as the error in the SO_2. Both the SO_2 and sulfate motivate the EUROPE_-CYCLE sensitivity test, in which we increase the seasonal cycle of European SO_2 emission (see section 4). Note that our results differ from those of *Feichter et al.* [1996], who had excessive wintertime SO_2 over Europe, and argued that their model needed either an additional oxidant or more vertical transport of SO_2 away from the surface. The annual cycle of wet deposition is captured quite well by the model, although the wet deposition in summer is somewhat under-estimated by the model. The deficient wet deposition in summer provides a possible explanation (at least in part) for the excessive modeled sulfate in that season.

[51] Is the deficient summer wet deposition related to a lack of summer rainfall? The final plot in Figure 11 shows the annual cycle of modeled and observed precipitation over the same region. The observations suggest that the modeled precipitation over Europe is somewhat deficient in summer. This may be because the model does not resolve the complex European topography. Note that although there is only a weak seasonal cycle in the modeled and observed total precipitation over Europe, there is a strong seasonal cycle in the convective component of the modeled precip-itation. This increases from 23% of the total precipitation in winter to 68% in summer. We found it necessary to include fairly efficient convective scavenging, including below-

cloud scavenging via (5), in order to obtain a reasonable match to the observed wet deposition in summer.

[52] Sulfate at high-latitude points is considered in Figure 12. At Jergul, the modeled sulfate is deficient in winter, despite the large modeled SO_2 values there. Further north at Bjørnøya, the modeled sulfate is deficient throughout the year. In Canada, the model again provides a good simulation at Cree Lake, but further north at Mould Bay the simulation of wintertime sulfate is deficient. This is also seen at Alert, in the far Canadian Arctic (not shown). A possible explanation for the deficient wintertime sulfate at the Arctic sites is a lack of SO_2 oxidation in ice clouds; this is discussed further when we consider the ICE_CLOUD_OX run in section 4. At the two Antarctic sites, the seasonal cycle is captured by the model, although its magnitude is much larger than in the observations. The simulation of sulfate at these points is sensitive to the (highly uncertain) emission of DMS from the ocean surface, and is improved when a different flux param-eterization is used (see section 4).

[53] Sulfate concentrations at six low-latitude oceanic sites are shown in Figure 13. Observations at marine sites in the Northern Hemisphere show strong seasonal enhancements of sulfate concentrations due to transport from the main anthro-pogenic source regions [*Andreae et al.*, 1988; *Savoie and Prospero*, 1989; *Savoie et al.*, 1989]. The summer maximum at Barbados is not picked up by the model, as was noted by *Chin et al.* [1996] for their model also. However, the spring-time maxima at Midway Island and Oahu are qualitatively
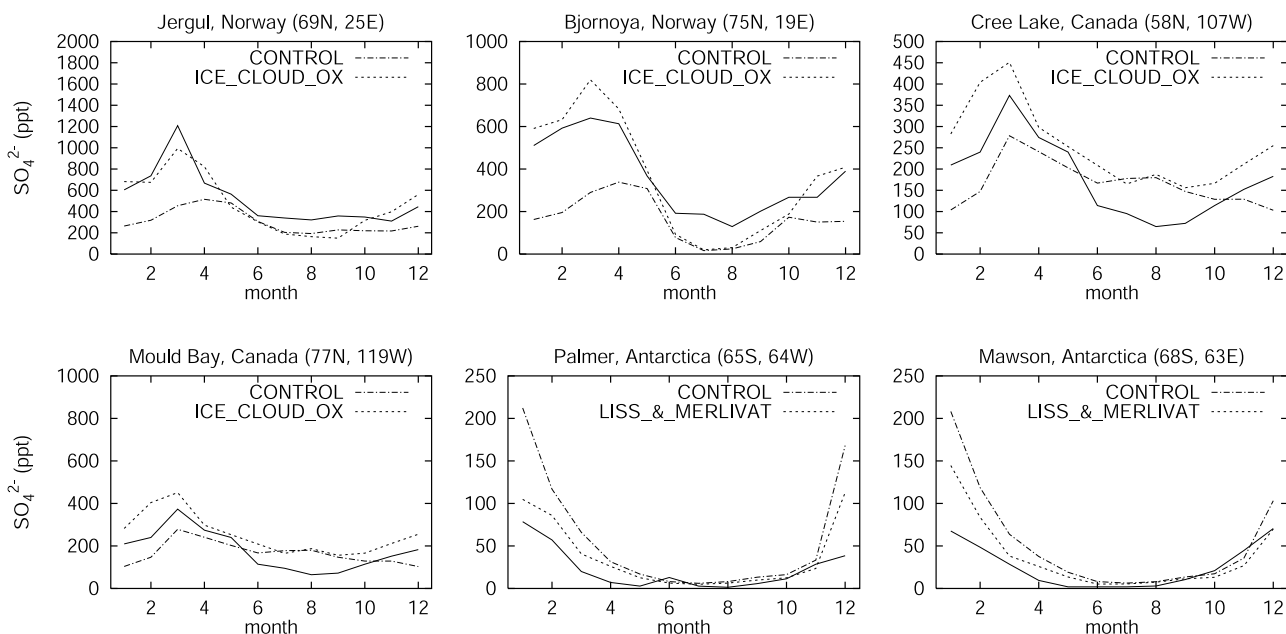
Figure 12. Seasonal variation of observed (solid lines) and modeled (dashed lines) monthly mean surface concentrations of sulfate at high-latitude sites. Observations are from EMEP for European sites and from *Chin et al.* [1996] and references therein for other sites. The ICE_CLOUD_OX and LISS_&_MERLIVAT runs are described in section 4.

captured by the model. According to *Huebert et al.* [2001], the springtime maximum in observed sulfate at Mauna Loa in Hawaii is due to transport from Asia; a similar maximum is seen at low altitude on Oahu. At Oahu, the model shows a second maximum in July, which appears to be related to excessive transport from North America.

[54] Surface observations at the Southern Hemisphere sites show somewhat lower concentrations than those at the Northern Hemisphere sites. The lack of a substantial seasonal cycle at American Samoa is captured by the model, but the mean modeled value is about half that observed. A possible explanation is excessive precipitation scavenging by the model in that area; the average modeled rainfall at that grid point is 9.7 mm per day, compared to a climatological value of 6.1 mm per day from *Huffman et al.* [1997]. If the model atmosphere is overly convective at this point, excessive
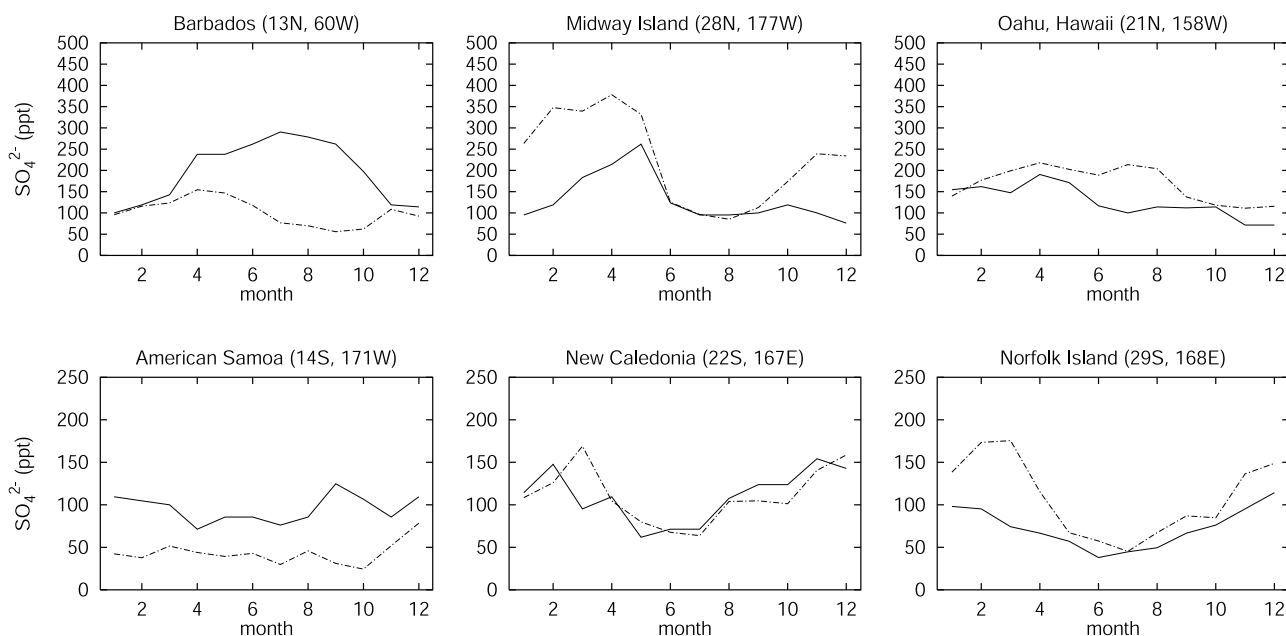
Figure 13. Seasonal variation of observed (solid lines) and modeled (dashed lines) monthly mean surface concentrations of sulfate at low-latitude oceanic sites. Observations are from *Chin et al.* [1996] and references therein.

mixing away from the surface would further exacerbate the situation. The seasonal cycle at New Caledonia, and to a lesser extent at Norfolk Island, is well captured by the model. The late summer maximum in the modeled sulfate concentrations at both of these points corresponds to a peak in the monthly mean emission of DMS, suggesting that the seasonal cycle is partly related to DMS chemistry.

4. Sensitivity Tests

[55] In this section, we explore some of the issues raised above through a number of sensitivity tests. For each of the sensitivity tests, we have repeated the run described above but with a single change to the model as described below. From each run, we have saved four years of data after the initial spinup period (rather than eight years as in the case of the CONTROL run).

4.1. SIMPLE_SCAV

[56] In this run, we return to a simpler treatment of wet scavenging, similar to that used in ECHAM4. In this treatment, large-scale in-cloud scavenging follows *Giorgi and Chameides* [1986], and below-cloud scavenging follows *Berge* [1993], with a collection efficiency of 0.1 for both sulfate and SO_2. The larger collection efficiency is expected to compensate, in average terms, for the lower scavenging rates given by the latter scheme (see section 2). However, in this run, below-cloud scavenging is applied only in cloud-free layers, and not in the clear portion of partly cloudy layers as in the CONTROL run. Below-cloud scavenging by snow is treated in the same way as rain. The collection efficiency for snow is thus 10 times larger than the value used for sulfate in the CONTROL run, and there is an additional term for below-cloud scavenging of SO_2 by snow, which is neglected in the CONTROL run. However, for sulfate, there is a compensating factor of 10 for the density of snow in the denominator of (6). In-cloud convective scavenging is retained as in the CONTROL run, but below-cloud scavenging by convective precipitation is neglected, as in the original implementation in ECHAM4.

[57] This run gives smaller scavenging rates and a larger sulfate burden. The latter increases from 0.67 Tg S to 0.93 Tg S, toward the higher end of the range of previous global simulations. The agreement with the observations over Europe is much worse in this run. The wet deposition of sulfur, averaged over the EMEP network, decreases from 805 to 661 mg S yr^{-1} (observed 882 mg S yr^{-1}). There is a corresponding increase in the surface sulfate concentration in that region from 1254 to 1678 ppt (observed 1259 ppt). A similar increase is obtained over the EMEFS network in North America: The average of the summer and winter surface sulfate concentrations increases from 1265 to 1530 ppt (observed 1073). On the other hand, the wet deposition of sulfur at the South Pole increases from 0.14 to 0.35 mg S yr^{-1}, improving the agreement with the observed value. This is probably because of the inclusion of below-cloud scavenging of SO_2 by snow in this run.

4.2. ICE_CLOUD_OX

[58] In this run, we consider the possibility that inclusion of oxidation in ice clouds could improve the simulation of SO_2 and sulfate in the Arctic. The CONTROL run had excessive SO_2 and deficient sulfate concentrations at the surface in winter, in common with a number of other models. During winter, clouds at these latitudes will be mainly composed of ice. Oxidation of SO_2 in ice clouds is not well understood, and is usually neglected in models, but laboratory experiments have confirmed that a reaction occurs between SO_2 and H_2O_2 in the presence of ice [*Mitra et al.*, 1990; *Conklin et al.*, 1993]. More recently, *Chu et al.* [2000] showed that sulfate is a major product of this reaction, and *Clegg and Abbatt* [2001] made a first estimate of the rate of this reaction as a function of the gas-phase abundances of SO_2 and H_2O_2. In the ICE_CLOUD_OX run, oxidation of SO_2 is permitted to occur in all stratiform clouds, including ice clouds. The ice water content in ice clouds is treated as a liquid water content for the purpose of the oxidation calculation. This treatment is likely to overestimate the real rate of oxidation in ice clouds.

[59] The wintertime simulation at high latitudes shows a large sensitivity to inclusion of this process. Results from the ICE_CLOUD_OX run for several Arctic and sub-Arctic sites are shown in Figures 9 and 12. At Jergul, there is little effect on the SO_2 simulation (which was satisfactory in the CONTROL run), but the simulation of sulfate in the winter and early spring is much improved. Further north, at Bjørnøya, the winter biases from the CONTROL run are removed and the model has overcompensated in both the SO_2 and sulfate concentrations. There is also a marked effect at Cree Lake in the Canadian sub-Arctic, although the simulation of SO_2 there in the ICE_CLOUD_OX run is worse than the good simulation in the CONTROL run. Further north, at Mould Bay, the simulation of sulfate is much improved for the first few months of the year in the ICE_CLOUD_OX run. However, in the Antarctic, the modeled sulfate concentrations, which are already too large in the CONTROL run, are even larger in the ICE_CLOUD_OX run (not shown).

4.3. LISS_&_MERLIVAT

[60] In this run, emission of DMS from the ocean surface was calculated following *Liss and Merlivat* [1986] instead of *Nightingale et al.* [2000]. The global DMS emission is reduced from 22.1 to 14.3 Tg S yr^{-1}. The DMS burden is reduced from 0.085 to 0.056 Tg S, and the sulfate burden is reduced from 0.67 to 0.61 Tg S. A marked weakening of the sulfur cycle is seen in remote regions. The SO_2 concentration for March–April between 55°S and 65°S decreases from 30 to 19 ppt, in better agreement with the observed value of 11 ppt. A better simulation of the seasonal cycle of sulfate is also obtained at the Antarctic sites (Figure 12). Evidently, the simulation in the Antarctic region is highly sensitive to the scheme used to calculate the DMS emission. In a recent model intercomparison [*Penner et al.*, 2001], DMS emission from the ocean surface was calculated as the average of the values from *Liss and Merlivat* [1986] and the larger values from *Wanninkhof* [1992], giving a global emission of 25.3 Tg S yr^{-1}. Most of the models that participated in that study had excessive sulfate at Palmer in the Antarctic.

[61] The seasonal cycles of modeled quantities from this run at Amsterdam Island and Cape Grim were shown in Figure 8, together with the observations and the modeled values from the CONTROL run. In the LISS_&_MERLI-

VAT run, the simulation of DMS during the summer is deficient at these sites, but the simulation of sulfate at Cape Grim is improved. Overall, there is a suggestion that the parameterization of *Liss and Merlivat* [1986] gives better overall agreement with the observations.

4.4. LINEAR_SLT

[62] It was suggested in section 3 that the model might not be transporting trace quantities away from the major source areas sufficiently quickly, especially in North America. It is known that higher-order methods of calculating advection may not perform well in the vicinity of steep gradients or discontinuities [e.g., *Durran*, 1999]. Therefore, a possible cause of the problem is that the horizontal gradients of tracer concentration are too steep for the bicubic interpolation used in the semi-Lagrangian horizontal advection scheme. While the scheme does truncate any resulting "overshoots" in the interpolated fields using the method of *Bermejo and Staniforth* [1992], this approach has not been rigorously tested for fields such as SO_2, which can exhibit large horizontal gradients. A related issue is the neglect of horizontal subgrid transports, which were included, for example, in the model of *Kasibhatla et al.* [1997]. These thoughts motivate another sensitivity test, in which we use simple bilinear interpolation to calculate the tracer mixing ratios at the departure points of the trajectories. In this run, denoted LINEAR_SLT, the interpolated value depends only on the values at the four surrounding grid points (instead of the 16-point algorithm used in the bicubic scheme). The linear scheme includes more numerical diffusion than the higher-order scheme; this is a general property of low- versus high-order schemes [e.g., *Durran*, 1999].

[63] In gross terms, the simulation does not look remarkably different in this run. For example, the global SO_2 burden reduces just slightly, from 0.42 to 0.41 Tg S. However, the wintertime SO_2 concentrations at the three points in the US Midwest discussed previously (Figure 9) are substantially reduced in this run, and agree better with the observations. The sulfate concentrations at these points (Figure 10) are less sensitive to the change of advection scheme, and there is only a modest improvement there in winter. The summertime sulfate concentrations are also slightly reduced in this run, and agree less well with the observed values. Still, this run shows the sensitivity of the modeled SO_2 in the source region to the choice of advection scheme, and suggests that further investigation is warranted.

4.5. EUROPE_CYCLE

[64] Although the results over Europe were satisfying in annual-mean terms, our model is typical of current models in that the seasonal cycle of sulfate is not well simulated there (Figure 11). According to *Chin et al.* [2000b], an explanation for the apparent underestimate in winter, as least in part, is the inclusion of sea-salt sulfate in the EMEP observations. In our model, both SO_2 and sulfate appear to be too large in summer, and too small in winter, suggesting that some improvement might be obtained by increasing the seasonal cycle in the SO_2 emissions over Europe. We have therefore performed a sensitivity test (denoted EUROPE_-CYCLE) in which we multiplied the monthly mean European anthropogenic SO_2 emissions by the ratio of the

observed to modeled SO_2 for each calendar month (where the modeled SO_2 is that from the CONTROL run, as shown in the first panel of Figure 11). The ratio reaches a maximum of 1.29 in March, and has minima of 0.74 and 0.73 in September and December respectively. As expected, the SO_2 seasonal cycle is much improved, but more importantly, the sulfate seasonal cycle is also improved (see Figure 11). Further improvement in the sulfate would be obtained in our model by correcting the summertime underestimate of wet deposition of sulfate, which appears to be at least partly related to a lack of summer rainfall. If justification could be found to increase the seasonal cycle of the European SO_2 emissions, then other models might also benefit from such an increase. Thus, it might not be necessary to include an additional oxidation pathway to achieve a reasonable simulation of the seasonal cycle of European sulfate.

4.6. NO_IMPACT_SCAV

[65] It has been suggested previously that below-cloud scavenging of sulfate is a relatively unimportant term [*Berge*, 1993]. In the NO_IMPACT_SCAV run, we turned off below-cloud scavenging of SO_2 and sulfate (by both stratiform and convective precipitation). The global SO_2 burden increased from 0.42 to 0.48 Tg S, and the global sulfate burden again increased from 0.67 to 0.93 Tg S. Thus, below-cloud scavenging has an important effect in our scheme, especially on sulfate. This is also seen over Europe and North America, where the surface sulfate concentrations averaged over the regions described in Table 3 increase to 1446 and 1494 ppt respectively. In both cases, this reduces the level of agreement with the observations.

4.7. Other Tests

[66] In the NO_DMS_FASTOX run, we removed the factor of two that was used to enhance the oxidation rate of DMS in the CONTROL run. The modeled DMS concentrations are very sensitive to this factor: The global burden of DMS increases from 0.085 Tg S in the CONTROL run to 0.14 Tg S in this run. This is larger than the DMS burdens obtained in most other global models [*Koch et al.*, 1999; *Rasch et al.*, 2000a], and close to the value of 0.15 Tg S from ECHAM4. More importantly, the agreement between the model and observed DMS at Amsterdam Island and Gape Grim is worse in this run. At Amsterdam Island, the annual-mean DMS concentration increases from 184 to 262 ppt (observed 182 ppt) and at Cape Grim, the annual-mean DMS concentration increases from 88 ppt to 151 ppt (observed 62 ppt). This suggests that either the enhanced oxidation rate is necessary to obtain a good simulation, or that the DMS emissions are too large in the model.

[67] In the DOUBLE_SCAV run, we increased the collection efficiency for below-cloud scavenging of SO_2 and sulfate by rain to 0.1, since this value is often used in GCMs. The global SO_2 burden decreased from 0.42 to 0.40 Tg S, and the global sulfate burden decreased from 0.67 to 0.55 Tg S. As expected, sulfate is more sensitive to this parameter than SO_2.

[68] In the NO_CONV_OX scheme, we turned off oxidation of SO_2 in convective clouds, because this process is often omitted in sulfur-cycle models. The global SO_2 burden increased from 0.42 to 0.52 Tg S, and the global

sulfate burden decreased from 0.67 to 0.59 Tg S. The sign of this result is model dependent. In the CSIRO model, convective transport and scavenging are calculated before the sulfur chemistry during each time step, so only the unscavenged SO_2 is subject to oxidation in convective clouds. By the next time step, the new sulfate is mixed uniformly throughout the grid box, so inclusion of SO_2 oxidation in convective clouds does not result in a large increase in convective scavenging of sulfate. *Lohmann et al.* [1999b] found that including oxidation of SO_2 in convective clouds reduced both SO_2 and sulfate, because of subsequent wet scavenging of sulfate. In that model, the convective scavenging occurred after the sulfur chemistry. This shows the potential sensitivity of model results to the order in which processes are applied.

[69] In the NO_SNOW_SCAV run, we turned off scavenging of sulfate by snow, because this process is sometimes omitted in models. Omission of this process has a modest effect on the global sulfate burden, increasing it from 0.67 to 0.69 Tg S. At points where frozen precipitation processes are dominant, the effect can be larger. For example, at the South Pole the annual-mean sulfate concentration increases from 31 to 43 ppt, in worse agreement with the observed value of 20 ppt.

5. Summary and Conclusions

[70] We have described and evaluated a treatment of the sulfur cycle that has recently been implemented in the CSIRO GCM. The treatments of chemistry, emissions and dry deposition were similar to those developed previously for the ECHAM4 model by *Feichter et al.* [1996] and *Lohmann et al.* [1999a]. The calculation of transport by advection, turbulent mixing and deep convection was developed independently, since the methods used to represent these processes are intrinsic to each climate model. We also completely rewrote the treatment of wet scavenging, to better reflect the different properties of liquid and frozen precipitation, and the treatment of these in the model's cloud microphysical scheme [*Rotstayn*, 1997; *Rotstayn et al.*, 2000]. Our scavenging scheme is more efficient than the simpler scheme from ECHAM4, and gives a smaller sulfate burden as well as more realistic (smaller) surface sulfate concentrations over Europe and North America. Thus, the treatment of wet scavenging may explain why ECHAM4 has a global sulfate burden at the higher end of results obtained with recent models [*Rasch et al.*, 2000a], and was found by *Huebert et al.* [2001] to overestimate sulfate concentrations relative to observations.

[71] Our scheme includes two physically based parameterizations for the removal of trace quantities by below-cloud scavenging, one for rain and one for snow. The parameterization for rain is nonlinear in the rainfall rate, because of the assumed Marshall–Palmer raindrop size distribution, and the increase of fallspeed with raindrop size. This differs from the linear approach used in some other global models. Our results show that there is a marked sensitivity to the assumed collection efficiency for sulfate by rain, and do not support the suggestion by *Berge* [1993] that below-cloud scavenging is a small term. This is in part because we have included this process in the clear air in partly cloudy layers. It is also because our parameterization

gives larger scavenging coefficients than the linearized form used by *Berge* [1993], especially at low rainfall rates. For a given collection efficiency and precipitation flux, our parameterization for below-cloud scavenging by snow yields larger scavenging coefficients than that for rain, because the assumed density of snowflakes is a factor of 10 lower than that of liquid water. On the other hand, the lower collection efficiency for snow reduces the impact of this difference.

[72] Although we paid considerable attention to the physical basis of the treatment of wet scavenging, many uncertainties exist. An indication of the large sensitivity of the simulation to the treatment of wet scavenging was provided by some of the sensitivity tests that were presented in section 4. One advantage of separating the treatments of scavenging by rain and snow, as in our scheme, is that it provides a suitable framework for testing the effects of perturbing various parameters, or including and excluding various processes. An example would be the scavenging of SO_2 in frozen precipitation, which was only included in our standard scheme when frozen precipitation forms by accretion (riming) of liquid water. However, it is straightforward to include the direct uptake of SO_2 on falling ice particles in the scheme, if evidence becomes available to indicate an appropriate value for the collection efficiency. It is encouraging that our scheme is able to provide a reasonable simulation of the annual cycle of wet deposition of nss-sulfur over Europe, in spite of the uncertainties.

[73] Our modeled concentrations of DMS, SO_2 and sulfate agreed with observed values to within a factor of two at most, but not all of the points sampled. In annual-mean terms, the results over Europe were more satisfactory than those over North America, where the modeled SO_2 and sulfate showed a high bias. Modeled concentrations in remote regions were generally reasonable, although there was a high bias in the modeled sulfate at Antarctic points. Sensitivity tests suggested possible explanations for some of the model biases. For example, we suggested that there was a lack of transport of trace quantities away from the most polluted regions in North America, and showed that there was a marked sensitivity there to the treatment of horizontal advection. We also noted the possibility of including a treatment of subgrid horizontal transport. The Antarctic results showed a large sensitivity to the calculation of DMS emission from the ocean surface, and better results were obtained there when we calculated this following *Liss and Merlivat* [1986] instead of *Nightingale et al.* [2000]. However, at lower latitudes the results were less clear-cut when comparing these two schemes.

[74] Another sensitivity test that gave an interesting result was the experiment in which we included oxidation of SO_2 in ice clouds. This process is not well understood, and is usually omitted in sulfur-cycle models, but laboratory experiments reviewed in the previous section confirm that such oxidation does occur. This run gave a much improved wintertime simulation of both SO_2 and sulfate in the Arctic, suggesting that this process should be studied further for possible inclusion in sulfur-cycle models in the future.

[75] We also showed that increasing the seasonal cycle of sulfur emission over Europe improved the simulation of both SO_2 and sulfate in that region. (In reaching this conclusion, we were careful to compare the model with

European observations that were averaged over a period centered on the year for which our emissions were derived.) Our results suggest that it may be possible to obtain a reasonable simulation of the annual cycle of European sulfate without the inclusion of additional reaction pathways. However, it may still be important to include additional pathways for the oxidation of SO_2 to sulfate, as discussed by some authors [e.g., *Feichter et al.*, 1996; *Kasibhatla et al.*, 1997]. Some pathways that may be important are the aqueous oxidation of SO_2 in sea-salt aerosol water [*Sievering et al.*, 1992, 1999], and the reaction of SO_2 on the surface of mineral aerosols [*Dentener et al.*, 1996]. This is an important topic for further research.

References

Adams, P. J., J. H. Seinfeld, and D. M. Koch, Global concentrations of tropospheric sulfate, nitrate and ammonimum aerosol simulated in a general circulation model, *J. Geophys. Res.*, *104*, 13,791–13,823, 1999.

Albrecht, B. A., Aerosols, cloud microphysics, and fractional cloudiness, *Science*, *245*, 1227–1230, 1989.

Andreae, M. O., H. Berresheim, T. W. Andreae, M. A. Kritz, T. S. Bates, and J. T. Merrill, Vertical distribution of dimethylsulfide, sulfur dioxide, aerosol ions, and radon over the northeast Pacific Ocean, *J. Atmos. Chem.*, *6*, 149–173, 1988.

Ayers, G. P., S. T. Bentley, J. P. Ivey, and B. W. Forgan, Dimethyl sulfide in marine air at Cape Grim, 41°S, *J. Geophys. Res.*, *100*, 21,013–21,021, 1995.

Barrie, L., et al., A comparison of large scale atmospheric sulphate aerosol models COSAM: Overview and highlights, *Tellus, Ser. B*, *53*, 615–645, 2001.

Barth, M. C., P. J. Rasch, J. T. Kiehl, C. M. Benkovitz, and S. E. Schwartz, Sulfur chemistry in the National Center for Atmospheric Research Community Climate Model: Description, evaluation, features, and sensitivity to aqueous chemistry, *J. Geophys. Res.*, *105*, 1387–1415, 2000.

Bates, T. S., J. D. Cline, R. H. Gammon, and S. R. Kelly-Hansen, Regional and seasonal variations in the flux of oceanic dimethylsulfide to the atmosphere, *J. Geophys. Res.*, *92*, 2930–2938, 1987.

Beheng, K. D., A parameterization of warm cloud microphysical conversion processes, *Atmos. Res.*, *33*, 193–206, 1994.

Benkovitz, C. M., M. T. Scholtz, J. Pacyna, L. Tarrason, J. Dignon, E. C. Voldner, P. A. Spiro, J. A. Logan, and T. E. Graedel, Global gridded inventories of anthropogenic emissions of sulfur and nitrogen, *J. Geophys. Res.*, *99*, 20,725–20,756, 1996.

Berge, E., Coupling of wet scavenging of sulphur to clouds in a numerical weather prediction model, *Tellus, Ser. B*, *45*, 1–22, 1993.

Bermejo, R., and A. Staniforth, The conversion of semi-Lagrangian advection schemes to quasi-monotone schemes, *Mon. Weather Rev.*, *120*, 2622–2632, 1992.

Berresheim, H., Biogenic sulfur emissions from the Subantarctic and Antarctic oceans, *J. Geophys. Res.*, *92*, 13,245–13,262, 1987.

Boucher, O., and U. Lohmann, The sulfate-CCN-cloud albedo effect. A sensitivity study with two general circulation models, *Tellus, Ser. B*, *47*, 281–300, 1995.

Chin, M., D. J. Jacob, G. M. Gardner, M. S. Foreman-Fowler, P. A. Spiro, and D. L. Savoie, A global three-dimensional model of tropospheric sulfate, *J. Geophys. Res.*, *101*, 18,667–18,690, 1996.

Chin, M., R. B. Rood, S.-J. Lin, J.-F. Müller, and A. M. Thompson, Atmospheric sulfur cycle simulated in the global model GOCART: Model description and global properties, *J. Geophys. Res.*, *105*, 24,671–24,687, 2000a.

Chin, M., D. L. Savoie, B. J. Huebert, A. R. Bandy, D. C. Thornton, T. S. Bates, P. K. Quinn, E. S. Saltzman, and W. J. De Bruyn, Atmospheric sulfur cycle simulated in the global model GOCART: Comparison with field observations and regional budgets, *J. Geophys. Res.*, *105*, 24,689–24,712, 2000b.

Chu, L., G. W. Diao, and L. T. Chu, Heterogeneous interaction of SO_2 on H_2O_2–ice films at 190–210 K, *J. Phys. Chem. A*, *104*, 7565–7573, 2000.

Chuang, C. C., J. E. Penner, K. E. Taylor, A. S. Grossman, and J. J. Walton, An assessment of the radiative effects of anthropogenic sulfate, *J. Geophys. Res.*, *102*, 3761–3778, 1997.

Clegg, S. M., and J. P. D. Abbatt, Oxidation of SO_2 by H_2O_2 on ice surfaces at 228 K: A sink for SO_2 in ice clouds, *Atmos. Chem. Phys.*, *1*, 73–78, 2001.

Conklin, M. H., R. A. Sommerfeld, S. K. Laird, and J. E. Villinski, Sulfur dioxide reactions on ice surfaces—Implications for dry deposition to snow, *Atmos. Environ.*, *27*, 2927–2934, 1993.

Dana, M. T., and J. M. Hales, Statistical aspects of the washout of polydisperse aerosols, *Atmos. Environ.*, *10*, 45–50, 1976.

Dentener, F., and P. J. Crutzen, A three-dimensional model of the global ammonia cycle, *J. Atmos. Chem.*, *19*, 331–369, 1994.

Dentener, F. J., G. R. Carmichael, Y. Zhang, J. Lelieveld, and P. J. Crutzen, Role of mineral aerosol as a reactive surface in the global troposphere, *J. Geophys. Res.*, *101*, 22,869–22,889, 1996.

Diehl, K., S. K. Mitra, and H. R. Pruppacher, A laboratory study on the uptake of HCl, HNO_3 and SO_2 gas by ice crystals and the effect of these gases on the evaporation rate of the crystals, *Atmos. Res.*, *48*, 235–244, 1998.

Durran, D. R., *Numerical Methods for Wave Equations in Geophysical Fluid Dynamics*, 482 pp., Springer-Verlag, New York, 1999.

Easter, R. C., and D. J. Luecken, A simulation of sulfur wet deposition and its dependence on the inflow of sulfur species to storms, *Atmos. Environ.*, *22*, 2715–2739, 1988.

Feichter, J., E. Kjellström, H. Rodhe, F. Dentener, J. Lelieveld, and G.-J. Roelofs, Simulation of the tropospheric sulfur cycle in a global climate model, *Atmos. Environ.*, *30*, 1693–1707, 1996.

Fowler, L. D., D. A. Randall, and S. A. Rutledge, Liquid and ice cloud microphysics in the CSU general circulation model, 1, Model description and simulated microphysical processes, *J. Clim.*, *9*, 489–529, 1996.

Ganzeveld, L., J. Lelieveld, and G.-J. Roelofs, A dry deposition parameterization for sulfur oxides in a chemistry and general circulation model, *J. Geophys. Res.*, *103*, 5679–5694, 1998.

Ghan, S., R. Easter, E. Chapman, H. Abdul-Razzak, Y. Zhang, L. Leung, N. Laulainen, R. Saylor, and R. Zaveri, A physically based estimate of radiative forcing by anthropogenic sulfate aerosol, *J. Geophys. Res.*, *106*, 5279–5293, 2001.

Ghan, S. J., L. R. Leung, and Q. Hu, Application of cloud microphysics to NCAR community climate model, *J. Geophys. Res.*, *102*, 16,507–16,527, 1997.

Giorgi, F., and W. L. Chameides, Rainout lifetimes of highly soluble aerosols and gases as inferred from simulations with a general circulation model, *J. Geophys. Res.*, *91*, 14,367–14,376, 1986.

Gordon, H. B., A flux formulation of the spectral atmospheric equations suitable for use in long term climate modeling, *Mon. Weather Rev.*, *109*, 56–64, 1981.

Graf, H., J. Feichter, and B. Langmann, Volcanic sulfur emissions: Estimates of source strength and its contribution to the global sulfate distribution, *J. Geophys. Res.*, *102*, 10,727–10,738, 1997.

Greenwald, T. J., G. L. Stephens, T. H. Vonder Haar, and D. L. Jackson, A physical retrieval of cloud liquid water over the global oceans using special sensor microwave/imager (SSM/I) observations, *J. Geophys. Res.*, *98*, 18,471–18,489, 1993.

Gregory, D., The representation of moist convection in atmospheric models, *Clim. Res. Tech. Note 54*, Hadley Cent., Bracknell, UK, 1995.

Gregory, D., and P. R. Rowntree, A mass flux convection scheme with representation of cloud ensemble characteristics and stability-dependent closure, *Mon. Weather Rev.*, *118*, 1483–1506, 1990.

Hao, W. M., M. H. Liu, and P. J. Crutzen, Estimates of annual and regional releases of CO_2 and other trace gases to the atmosphere from fires in the tropics, based on the FAO statistics for the period 1975–1980, in *Fire in the Tropical Biota. Ecosystem Processes and Global Challenges*, edited by J. G. Goldammer, pp. 440–462, Springer-Verlag, New York, 1990.

Haywood, J., and O. Boucher, Estimates of the direct and indirect radiative forcing due to tropospheric aerosols: A review, *Rev. Geophys.*, *38*, 513–543, 2000.

Hegg, D. A., P. V. Hobbs, and L. F. Radke, Measurements of the scavenging of sulfate and nitrate in clouds, *Atmos. Environ.*, *18*, 1939–1946, 1984.

Holtslag, A. A. M., and B. A. Boville, Local versus non-local boundary layer diffusion in a global climate model, *J. Clim.*, *6*, 1825–1842, 1993.

Huebert, B. J., C. A. Phillips, L. Zhuang, E. Kjellström, H. Rodhe, J. Feichter, and C. Land, Long-term measurements of free-tropospheric sulfate at Mauna Loa: Comparison with global model simulations, *J. Geophys. Res.*, *106*, 5479–5492, 2001.

Huffman, G. J., et al., The Global Precipitation Climatology Project (GPCP) combined precipitation dataset, *Bull. Am. Meteorol. Soc.*, *78*, 5–20, 1997.

Hynes, A. J., P. H. Wine, and D. J. Semmes, Kinetics and mechanisms of

OH reactions with organic sulfides, *J. Phys. Chem.*, *90*, 4148–4156, 1986.

Iribarne, J. V., T. Pyshnov, and B. Naik, The effect of freezing on the composition of supercooled droplets, 2, Retention of S(IV), *Atmos. Environ.*, *24A*, 389–398, 1990.

Jakob, C., and S. A. Klein, A parametrization of the effects of cloud and precipitation overlap for use in general-circulation models, *Q. J. R. Meteorol. Soc.*, *126*, 2525–2544, 2000.

James, J. D., R. M. Harrison, N. H. Savage, A. G. Allen, J. L. Grenfell, B. J. Allan, J. M. C. Plane, C. N. Hewitt, B. Davison, and L. Robertson, Quasi-Lagrangian investigation into dimethyl sulfide oxidation in maritime air using a combination of measurements and model, *J. Geophys. Res.*, *105*, 26,379–26,392, 2000.

Jones, A., D. L. Roberts, M. J. Woodage, and C. E. Johnson, Indirect sulphate aerosol forcing in a climate model with an interactive sulfur cycle, *J. Geophys. Res.*, *106*, 20,293–20,310, 2001.

Jylhä, K., Relationship between the scavenging coefficient for pollutants in precipitation and the radar reflectivity factor, 1, Derivation, *J. Appl. Meteorol.*, *38*, 1421–1434, 1999.

Kasibhatla, P., W. L. Chameides, and J. St. John, A three-dimensional global model investigation of seasonal variations in the atmospheric burden of anthropogenic sulfate aerosols, *J. Geophys. Res.*, *102*, 3737–3759, 1997.

Kettle, A. J., and M. O. Andreae, Flux of dimethylsulfide from the oceans: A comparison of updated data sets and flux models, *J. Geophys. Res.*, *105*, 26,793–26,808, 2000.

Kettle, A. J., et al., A global database of sea surface dimethylsulfide (DMS) measurements and a procedure to predict sea surface DMS as a function of latitude, longitude and month, *Global Biogeochem. Cycles*, *13*, 399–444, 1999.

Koch, D., D. Jacob, I. Tegen, D. Rind, and M. Chin, Tropospheric sulfur simulation and sulfate direct radiative forcing in the Goddard Institute for Space Studies general circulation model, *J. Geophys. Res.*, *104*, 23,799–23,822, 1999.

Langner, J., and H. Rodhe, A global three-dimensional model of the tropospheric sulfur cycle, *J. Atmos.Chem.*, *13*, 225–263, 1991.

Legrand, M., and R. J. Delmas, The ionic balance of Antarctic snow, a 10-yr detailed record, *Atmos. Environ.*, *18*, 1867–1874, 1984.

Lelieveld, J., G. J. Roelofs, J. Feichter, and H. Rodhe, Terrestrial sources and distribution of atmospheric sulphur, *Philos. Trans. R. Soc. London, Ser. B*, *352*, 149–158, 1997.

Liss, P. S., and L. Merlivat, Air–sea gas exchange rates: Introduction and synthesis, in *The Role of Air–Sea Gas Exchange in Geochemical Cycling*, edited by P. B. Menard, pp. 113–127, D. Reidel, Norwell, Mass., 1986.

Lohmann, U., and J. Feichter, Impact of sulfate aerosols on albedo and lifetime of clouds: A sensitivity study with the ECHAM4 GCM, *J. Geophys. Res.*, *102*, 13,685–13,700, 1997.

Lohmann, U., J. Feichter, C. C. Chuang, and J. E. Penner, Prediction of the number of cloud droplets in the ECHAM GCM, *J. Geophys. Res.*, *104*, 9169–9198, 1999a.

Lohmann, U., K. von Salzen, N. McFarlane, H. G. Leighton, and J. Feichter, Tropospheric sulfur cycle in the Canadian general circulation model, *J. Geophys. Res.*, *104*, 26,833–26,858, 1999b.

Lohmann, U., J. Feichter, J. E. Penner, and R. Leaitch, Indirect effect of sulfate and carbonaceous aerosols: A mechanistic treatment, *J. Geophys. Res.*, *105*, 12,193–12,206, 2000.

Lohmann, U., et al., Vertical distributions of sulfur species simulated by large scale atmospheric models in COSAM: Comparison with observations, *Tellus, Ser. B*, *53*, 646–672, 2001.

Louis, J.-F., A parametric model of vertical eddy fluxes in the atmosphere, *Boundary Layer Meteorol.*, *17*, 187–202, 1979.

Mari, C., D. J. Jacob, and P. Bechtold, Transport and scavenging of soluble gases in a deep convectivecloud, *J. Geophys. Res.*, *105*, 22,255–22,267, 2000.

Marshall, K. S., and W. M. Palmer, The distribution of raindrops with size, *J. Meteorol.*, *5*, 165–166, 1948.

McGregor, J. L., Economical determination of departure points for semi-Lagrangian models, *Mon. Weather Rev.*, *121*, 221–230, 1993.

McNaughton, D. J., and R. J. Vet, Eulerian model evaluation field study (EMEFS): A summary of surface network measurements and data quality, *Atmos. Environ.*, *30*, 227–238, 1996.

Mitra, S. K., S. Barth, and H. R. Pruppacher, A laboratory study of the scavenging of SO_2 by snow crystals, *Atmos. Environ., Ser. A*, *24*, 2307–2312, 1990.

Nguyen, B. C., N. Mihalopoulos, J. P. Putaud, A. Gaudry, L. Gallet, W. C. Keene, and J. N. Galloway, Covariations in oceanic dimethyl sulfide, its oxidation products and rain acidity at Amsterdam Island in the Southern Indian Ocean, *J. Atmos. Chem.*, *15*, 39–53, 1992.

Nightingale, P. D., G. Malin, C. S. Law, A. J. Watson, P. S. Liss, M. I. Liddicoat, J. Boutin, and R. C. Upstill-Goddard, In situ evaluation of air–

sea gas exchange parameterizations using novel conservative and volatile tracers, *Global Biogeochem. Cycles*, *14*, 373–387, 2000.

O'Farrell, S. P., Investigation of the dynamic sea ice component of a coupled atmosphere–sea ice general circulation model, *J. Geophys. Res.*, *103*, 15,751–15,782, 1998.

Penner, J. E., C. A. Atherton, and T. E. Graedel, Global emissions and models of photochemically active compounds, in *Global Atmospheric–Biospheric Chemistry*, edited by R. Prinn, pp. 223–248, Plenum, New York, 1994.

Penner, J. E., et al., Aerosols, their direct and indirect effects, in *Climate Change 2001: The Scientific Basis. Contribution of Working Group I to the Third Assessment Report of the Intergovernmental Panel on Climate Change (IPCC)*, edited by J. T. Houghton, Y. Ding, D. J. Griggs, M. Noguer, P. J. van der Linden, X. Dai, K. Maskell, and C. A. Johnson, pp. 289–348, Cambridge Univ. Press, New York, 2001.

Pham, M., J. F. Müller, G. P. Brasseur, C. Granier, and G. Mégie, A three-dimensional study of the tropospheric sulphur cycle, *J. Geophys. Res.*, *100*, 26,061–26,092, 1995.

Pruppacher, H. R., and J. D. Klett, *Microphysics of Clouds and Precipitation*, 2nd ed., 954 pp., Kluwer Acad., Norwell, Mass., 1997.

Radke, L. F., P. V. Hobbs, and M. W. Eltgroth, Scavenging of aerosol particles by precipitation, *J. Appl. Meteorol.*, *19*, 715–722, 1980.

Rasch, P. J., and J. E. Kristjánsson, A comparison of the CCM3 model climate using diagnosed and predicted condensate parameterizations, *J. Clim.*, *11*, 1587–1614, 1998.

Rasch, P. J., M. C. Barth, J. T. Kiehl, S. E. Schwartz, and C. M. Benkovitz, A description of the global sulfur cycle and its controlling processes in the National Center for Atmospheric Research Community Climate Model, Version 3, *J. Geophys. Res.*, *105*, 1367–1385, 2000a.

Rasch, P. J., et al., A comparison of scavenging and deposition processes in global models: Results from the WCRP Cambridge Workshop of 1995, *Tellus, Ser. B*, *52*, 1025–1056, 2000b.

Roelofs, G.-J., A cloud chemistry sensitivity study and comparison of explicit and bulk cloud model performance, *Atmos. Environ., Part A*, *27*, 2255–2264, 1993.

Roelofs, G.-J., J. Lelieveld, and L. Ganzeveld, Simulation of global sulfate distribution and the influence on effective cloud drop radii with a coupled photochemistry–sulfur cycle model, *Tellus*, *50B*, 224–242, 1998.

Roelofs, G.-J., et al., Analysis of regional budgets of sulfur species modeled for the COSAM exercise, *Tellus, Ser. B*, *53*, 673–694, 2001.

Rogers, R. R., and M. K. Yau, *A Short Course in Cloud Physics*, 3rd ed., 293 pp., Pergamon, New York, 1988.

Rossow, W. B., A. W. Walker, D. E. Beuschel, and M. D. Roiter, International Satellite Cloud Climatology Project (ISCCP) documentation of new cloud datasets, *WMO/TD No. 737*, 115 pp., World Meteorol. Organ., Geneva, 1996.

Rotstayn, L. D., A physically based scheme for the treatment of stratiform clouds and precipitation in large-scale models, 1, Description and evaluation of the microphysical processes, *Q. J. R. Meteorol. Soc.*, *123*, 1227–1282, 1997.

Rotstayn, L. D., Indirect forcing by anthropogenic aerosols: A global climate model calculation of the effective-radius and cloud-lifetime effects, *J. Geophys. Res.*, *104*, 9369–9380, 1999.

Rotstayn, L. D., and U. Lohmann, Tropical rainfall trends and the indirect aerosol effect, *J. Clim.*, *15*, 2103–2116, 2002.

Rotstayn, L. D., B. F. Ryan, and J. J. Katzfey, A scheme for calculation of the liquid fraction in mixed-phase stratiform clouds in large-scale models, *Mon. Weather Rev.*, *128*, 1070–1088, 2000.

Saltzman, E. S., D. B. King, K. Holmen, and C. Leck, Experimental determination of the diffusion coefficient of dimethylsulfide in water, *J. Geophys. Res.*, *98*, 16,481–16,486, 1993.

Savoie, D. L., and J. M. Prospero, Comparison of oceanic and continental sources of non-sea-salt sulfate over the Pacific Ocean, *Nature*, *339*, 685–687, 1989.

Savoie, D. L., J. M. Prospero, and E. S. Saltzman, Non-sea-salt sulfate and nitrate in trade wind aerosols at Barbados: Evidence for long-range transport, *J. Geophys. Res.*, *94*, 5069–5080, 1989.

Savoie, D. L., J. M. Prospero, R. Larsen, F. Huang, M. Izaguirre, T. Huang, T. H. Snowdon, L. Custals, and C. G. Sanderson, Nitrogen and sulfur species in Antarctic aerosols at Mawson, Palmer Station, and Marsh (King George Island), *J. Atmos. Chem.*, *17*, 95–122, 1993.

Schaug, J., J. E. Hansen, K. Nodop, B. Ottar, and J. M. Pacyna, Summary report from the chemical co-ordinating center for the third phase of EMEP, *Rep. 3/87*, 160 pp., EMEP/CCC, Norw. Inst. for Air Res., Lillestrom, 1987.

Sciare, J., N. Mihalopoulos, and F. J. Dentener, Interannual variability of atmospheric dimethylsulfide in the southern Indian Ocean, *J. Geophys. Res.*, *105*, 26,369–26,377, 2000.

Scott, B. C., Parameterization of sulfate removal by precipitation, *J. Appl. Meteorol.*, *17*, 1375–1389, 1978.

Seinfeld, J. H., and S. N. Pandis, *Atmospheric Chemistry and Physics: From Air Pollution to Climate Change*, 1326 pp., John Wiley, New York, 1998.

Sievering, H., J. Boatman, E. Gorman, Y. Kim, L. Anderson, G. Ennis, M. Luria, and S. Pandis, Removal of sulfur from the marine boundary layer by ozone oxidation in sea-salt aerosols, *Nature*, *360*, 571–573, 1992.

Sievering, H., B. Lerner, J. Slavich, J. Anderson, M. Posfai, and J. Cainey, O_3 oxidation of SO_2 in sea-salt aerosol water: Size distribution of non-sea-salt sulfate during the First Aerosol Characterization Experiment (ACE 1), *J. Geophys. Res.*, *104*, 21,707–21,717, 1999.

Spiro, P. A., D. J. Jacob, and J. A. Logan, Global inventory of sulfur emissions with $1° \times 1°$ resolution, *J. Geophys. Res.*, *97*, 6023–6036, 1992.

Sundqvist, H., A parameterization scheme for non-convective condensation including prediction of cloud water content, *Q. J. R. Meteorol. Soc.*, *104*, 677–690, 1978.

Tiedtke, M., Representation of clouds in large-scale models, *Mon. Weather Rev.*, *121*, 3040–3061, 1993.

Tripoli, G. J., and W. R. Cotton, A numerical investigation of several factors contributing to the observed variable intensity of deep convection over south Florida, *J. Appl. Meteorol.*, *19*, 1037–1063, 1980.

Tuncel, G., N. K. Aras, and W. H. Zoller, Temporal variations and sources of elements in the South Pole atmosphere, 1, Nonenriched and moderately enriched elements, *J. Geophys. Res.*, *94*, 13,025–13,038, 1989.

Twomey, S., The influence of pollution on the shortwave albedo of clouds, *J. Atmos. Sci.*, *34*, 1149–1152, 1977.

Van Leer, B., Towards the ultimate conservative difference scheme, 5, A new approach to numerical convection, *J. Comp. Phys.*, *23*, 276–299, 1977.

Wanninkhof, R., Relationship between wind speed and gas exchange over the ocean, *J. Geophys. Res.*, *97*, 7373–7382, 1992.

Weng, F., and N. C. Grody, Retrieval of cloud liquid water using the Special Sensor Microwave Imager (SSM/I), *J. Geophys. Res.*, *99*, 25,535–25,551, 1994.

Williams, K. D., A. Jones, D. L. Roberts, C. A. Senior, and M. J. Woodage, The response of the climate system to the indirect effects of anthropogenic sulfate aerosol, *Clim. Dyn.*, *17*, 845–856, 2001.

Wilson, D. R., and S. P. Ballard, A microphysically based precipitation scheme for the UK Meteorological Office Unified Model, *Q. J. R. Meteorol. Soc.*, *125*, 1607–1636, 1999.

Wojcik, G. S., and J. S. Chang, A re-evaluation of sulfur budgets, lifetimes, and scavenging ratios for eastern North America, *J. Atmos. Chem.*, *26*, 109–145, 1997.

————————————

U. Lohmann, Department of Physics and Atmospheric Science, Dalhousie University, Halifax, Nova Scotia, Canada.

L. D. Rotstayn, Division of Atmospheric Research, CSIRO, Private Bag 1, Aspendale, Victoria 3195, Australia. (leon.rotstayn@csiro.au)